



---

# **Overview of Image-Based Near Field-to-Far Field Transformations (NFFFTs)**

**April 2, 2008**

**Scott A. Rice**

**Michigan Research and Development Center (MRDC)**

**General Dynamics Advanced Information Systems**

**scott.rice@gd-ais.com**

**© Copyright 2008 General Dynamics Advanced Information Systems**



# NFFFT Outline

## ➔ NFFFT Overview

- Background and formulation
- Collection geometries

## Example CNFFFT Results

- RCS statistics
- Position error sensitivity
- Antenna pattern compensation
- Sub-360° processing

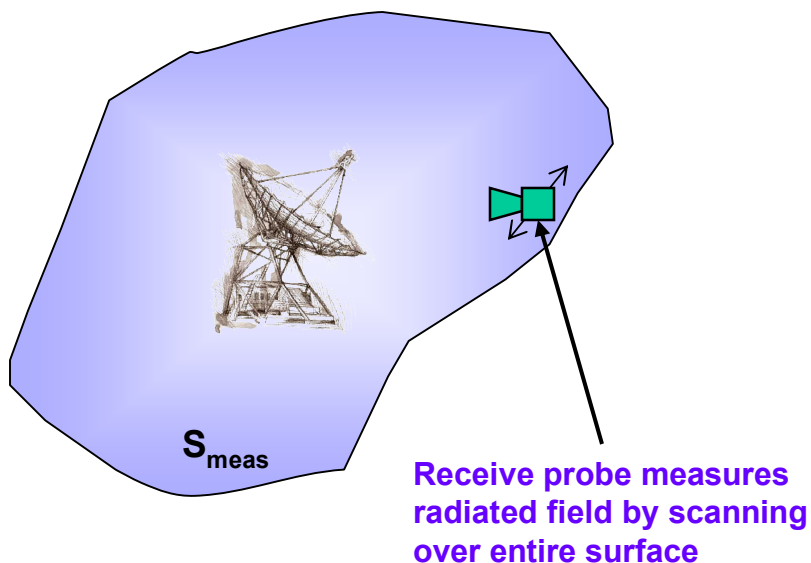
## Summary

***Not-So-Recent Overview of historical GD-AIS NFFFT work:***

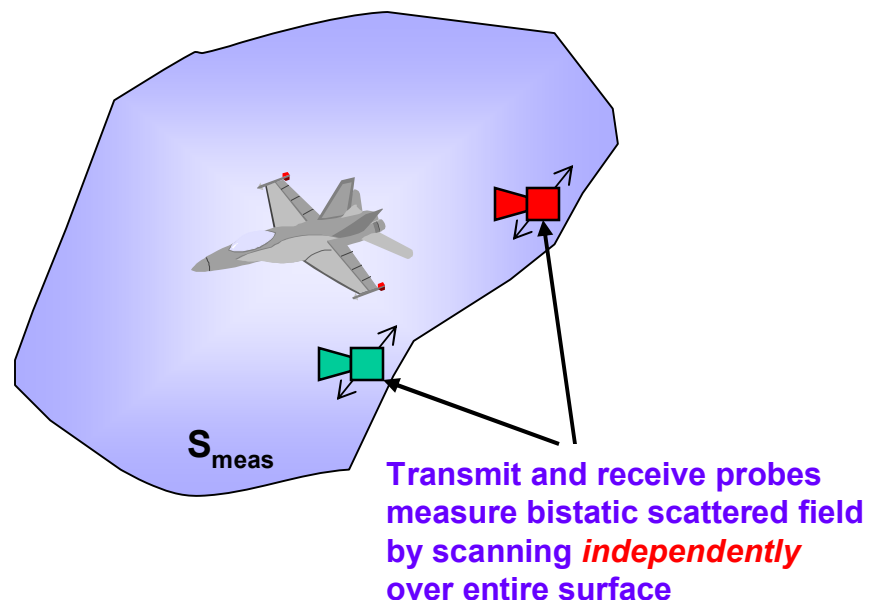
*LaHaie, I.J. (2003), "Overview of an Image-Based Technique for Predicting Far Field Radar Cross-Section From Near Field Measurements," IEEE Ant. Prop. Mag., Vol. 45, No. 6, pp. 159-169.*

# Rigorous Near Field Transformations

## Near Field Antenna Measurements



## Near Field Scattering Measurements



- Rigorous EM theory says that knowledge of a *radiated field* on a closed surface surrounding a source (antenna) implies knowledge everywhere in space (including the far field)
  - spheres and planes (and cylinders) allow wave function expansions for fast transformations
  - equivalent to synthesizing a plane wave
- Unfortunately, for *scattering* measurements (RCS), this theory applies *separately* to the incident and scattered fields – *bistatic* measurements are needed
  - must synthesize both the incident and scattered plane waves
  - provides full bistatic output (even if only monostatic is needed)

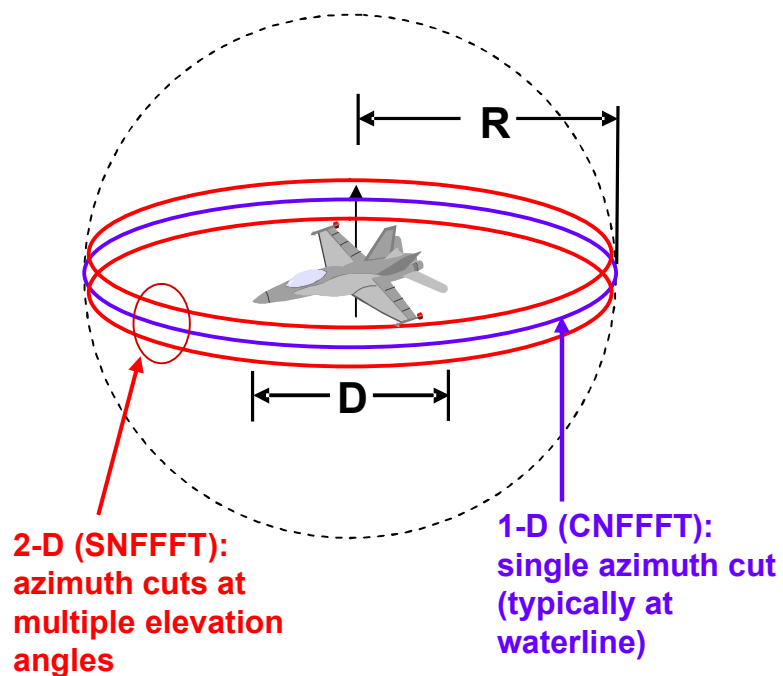


# Image-Based NFFFT Background

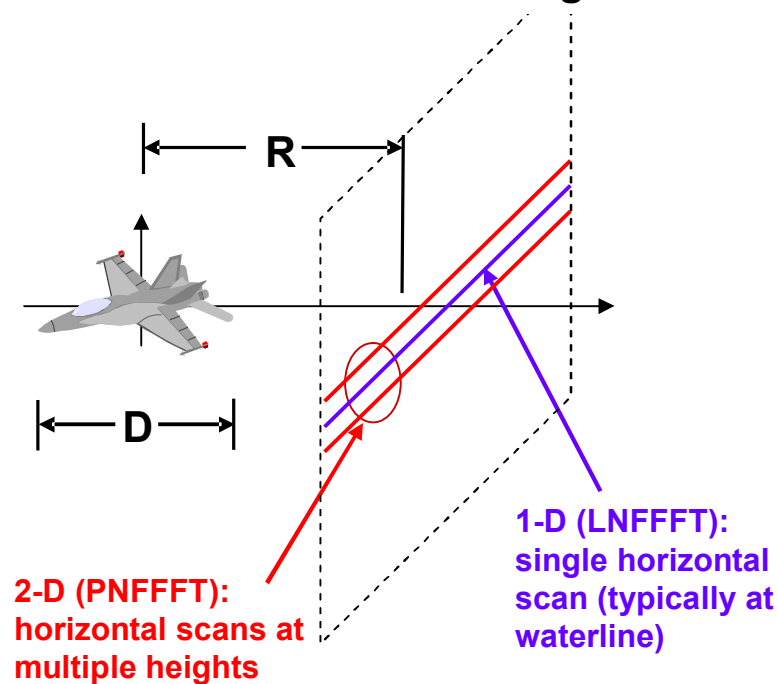
- GDAIS MRDC has developed a collection of near field-to-far field transformation (NFFFT) algorithms for *monostatic* RCS measurements
  - Based upon scalar SAR imaging (single scattering) model
  - The term “image-based” in the name is a reference to the SAR scattering model, *not* an implicit requirement to form an image
  
- NFFFT has demonstrated very good far field prediction performance for both *RCS patterns* and *RCS sector statistics* (mean, median,  $P_{cum}$ ) as a function of frequency, standoff distance, and target geometry
  - primary limitation is multiple scattering (interactions)
    - results in misalignment of peaks and nulls (overall level is less affected)
    - statistics of NFFFT predictions are often more accurate than patterns themselves
    - not an issue if interactions are locally in the far field

# NFFFT Collection Geometries

## Spherical / Circular Scanning



## Planar / Linear Scanning



- **2-D scanning:** required for targets having NF effects in all three dimensions
  - treated as a full 3-D scattering problem
- **1-D scanning:** sufficient for FF waterline RCS of targets where "out-of-plane" NF effects are negligible
  - typically the vertical direction
  - treated as an equivalent 2-D scattering problem
- In all cases, wideband measurements are required

# Generic NFFFT Fundamentals – 1 of 3

## How to Beat the “Bistatic” Dilemma...

### The Model

- Assume target satisfies scalar SAR “reflectivity density” model
  - implies multiple interactions are small or localized

### Near Field Measurement

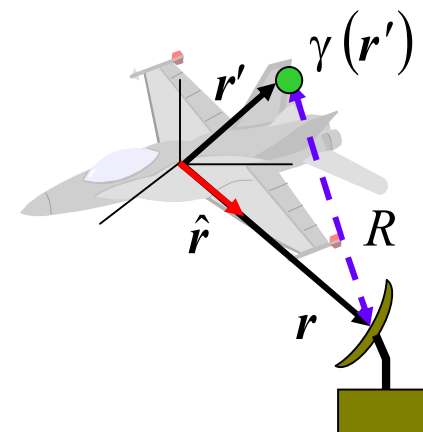
$$u(\mathbf{r}, k) = C \int_V \gamma(\mathbf{r}') \frac{e^{i2kR}}{(4\pi R)^2} d\mathbf{r}'$$

2-way spherical wave

### Far Field Scattering Pattern

$$S_{FF}(\hat{\mathbf{r}}, k) = \frac{1}{4\pi} \int_V \gamma(\mathbf{r}') e^{-i2k\hat{\mathbf{r}} \cdot \mathbf{r}'} d\mathbf{r}'$$

2-way plane wave



### The Observation

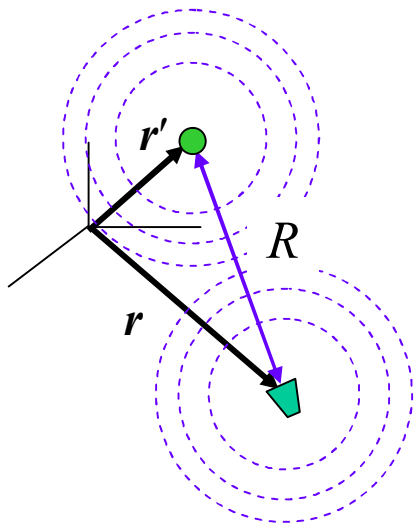
- Far field kernel is in the form of a propagating wave (a plane wave at twice the frequency)
  - but the near field kernel is not
- If only we could represent the near field kernel as a propagating wave...
  - we could then relate the near field to the far field

# Generic NFFFT Fundamentals – 2 of 3

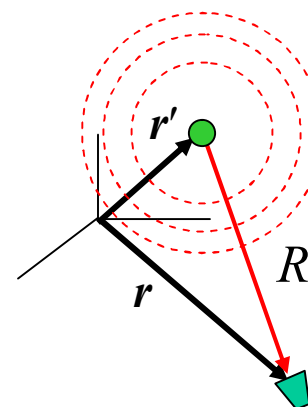
## The "Trick"

- Apply a range-dependent weighting to the near field data

Actual Near Field Measurement



Modified Near Field Measurement



2-way kernel

$$\frac{e^{i2kR}}{(4\pi R)^2}$$

Frequency FFT  
(Range Profile)

x R (2-D scan)

x R<sup>3/2</sup> (1-D scan)

Range  
Compensation

Range IFFT

1-way kernels

$$\left\{ \begin{array}{l} \frac{e^{i2kR}}{4\pi R} \\ \frac{e^{i2kR}}{\sqrt{i\pi kR}} \propto H_0^{(1)}(2kR) \end{array} \right.$$

- Near field kernel now satisfies the 3-D or 2-D propagating wave (spherical/cylindrical wave)



# Generic NFFFT Fundamentals – 3 of 3

## Preprocessed (Modified) NF Data

$$U'(\mathbf{r}, k) \left\{ \begin{array}{l} = C' \int_V \gamma(\mathbf{r}') \frac{e^{i2kR}}{4\pi R} d\mathbf{r}' \quad \leftarrow \text{2-D scan (spherical, planar)} \\ \approx C' \int_V \gamma(\mathbf{r}') H_0^{(1)}(2kR) d\mathbf{r}' \quad \leftarrow \text{1-D scan (circular, linear)} \end{array} \right.$$

## The Rest

- Expand near field kernel into a summation of 3-D or 2-D outward-traveling waves (exponentials) originating from the origin of coordinates
  - a Fourier transform can typically be used to efficiently compute this expansion
- Multiply each near field component wave by a factor to convert it to the corresponding far field component
- Sum up the far field components (exponentials) to get the far field data
  - can typically be done with inverse Fourier transforms

# The Math\* is obvious...

## Preprocessed Nearfield Data:

$$U'(\phi, k) = \frac{1}{(4\pi)^2} \sqrt{\frac{i\pi k}{\rho_c}} \iint \gamma(\rho', \phi') \frac{e^{i2kR}}{\sqrt{i\pi k R}} \rho' d\rho' d\phi'$$

$$\approx \frac{1}{(4\pi)^2} \sqrt{\frac{i\pi k}{\rho_c}} \iint \gamma(\rho', \phi') H_0^{(1)}(2kR) \rho' d\rho' d\phi'$$

## Far-Field Scattering Pattern:

$$S_{FF}(\phi, k) = \frac{1}{4\pi} \int_V \gamma(\rho', \phi') e^{-i2k\rho' \cos(\phi - \phi')} \rho' d\rho' d\phi'$$

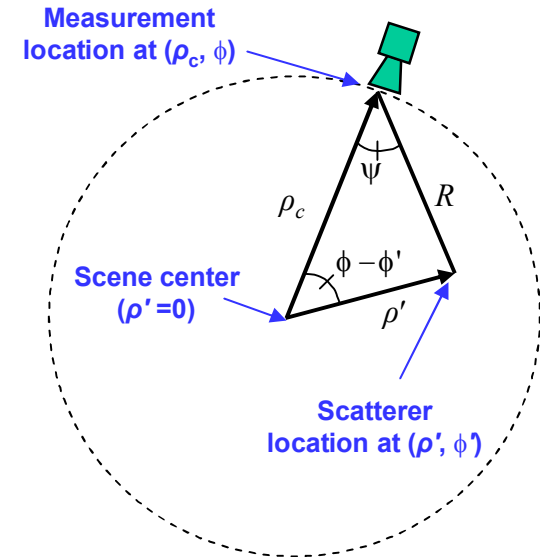
## Cylindrical Wave Expansions:

$$H_0^{(1)}(2kR) = \sum_{n=-\infty}^{\infty} H_n^{(1)}(2k\rho_c) J_n(2k\rho') e^{in(\phi - \phi')}$$

$$e^{-i2k\rho' \cos(\phi - \phi')} = \sum_{n=-\infty}^{\infty} (-i)^n J_n(2k\rho') e^{-in(\phi - \phi')}$$

## CNFFFT Far-Field Scattering Pattern Estimate:

$$S_{FF}(\phi, k) = 2 \sqrt{\frac{\rho_c}{i\pi k}} \sum_{n=-N}^N \frac{(-i)^n e^{in\phi}}{H_n^{(1)}(2k\rho_c)} \int_0^{2\pi} U'(\phi, k) e^{-in\phi} d\phi$$



Combine

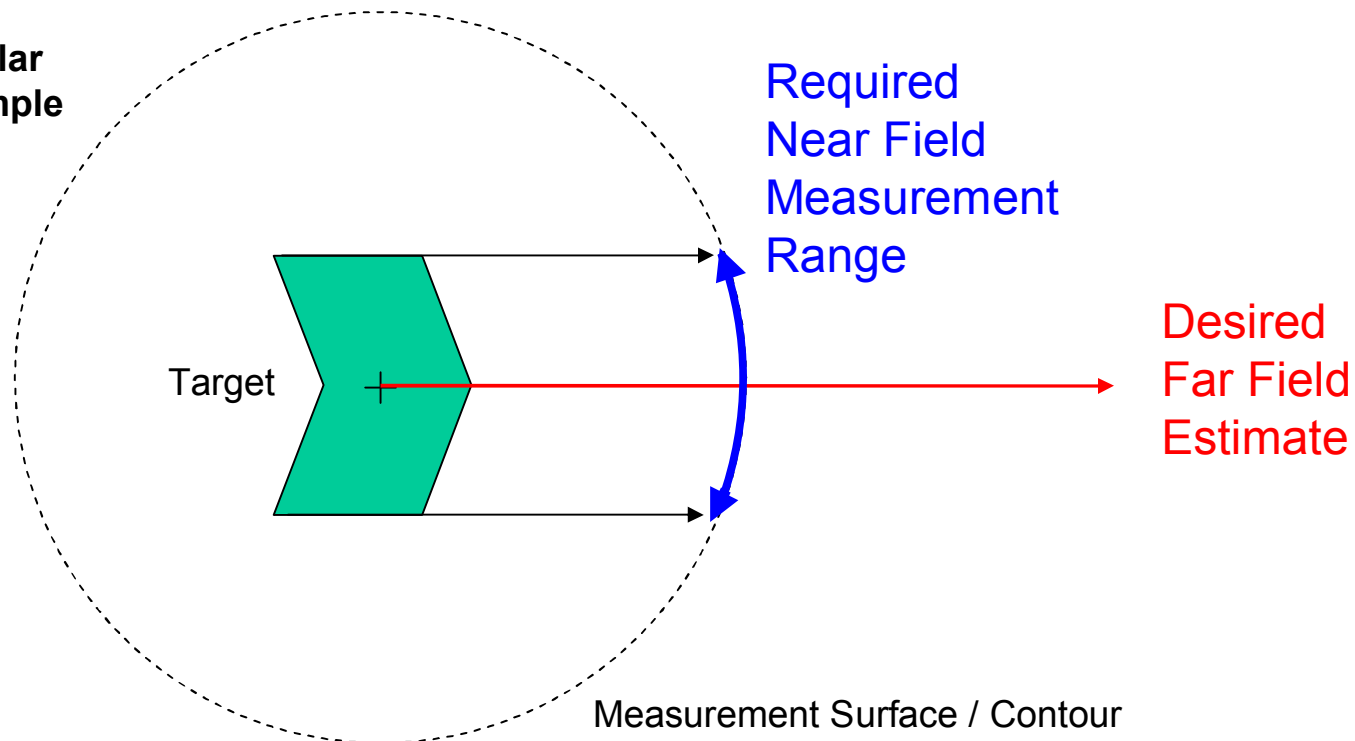
\* LaHaie, I. J., et al. (2005), "An Improved Version of the Circular Near Field-to-Far Field Transformation (CNFFFT)," *Proc. AMTA '05*, pp. 196-201.

# NFFFT Measurement Requirements

## Minimum Sample Region Concept

- **As a minimum**, NF measurements must span the projection of target onto scan surface/contour along desired FF directions for accurate RCS prediction
  - applies to both 2-D or 1-D scans
  - independent of NFFFT algorithm

1-D Circular  
Scan Example





# Outline

## NFFFT Overview

- Background and formulation
- Collection geometries

## → Example CNFFFT Results

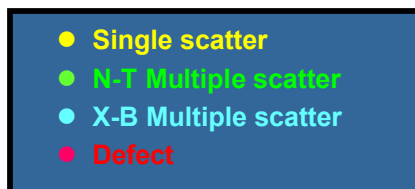
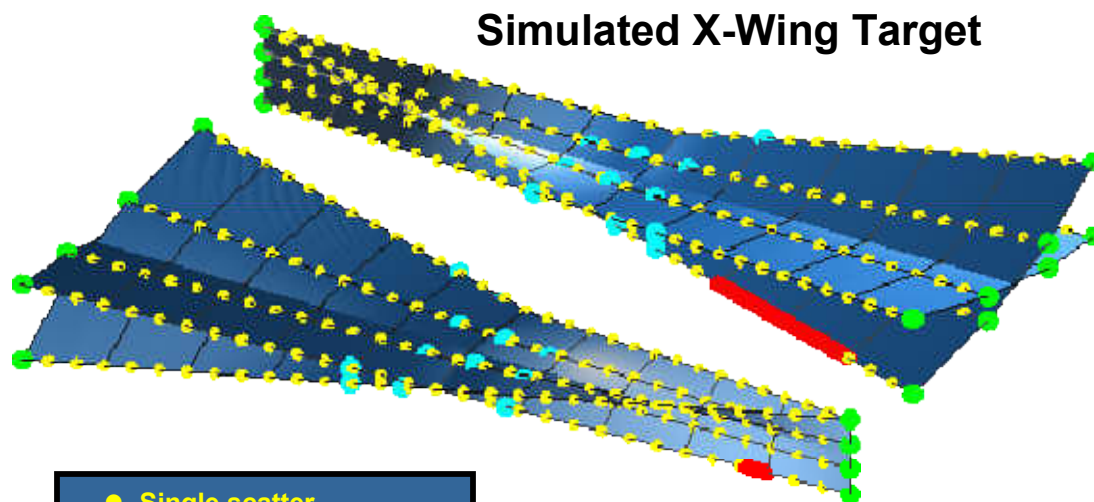
- ■ RCS statistics
  - Position error sensitivity
  - Antenna pattern compensation
  - Sub-360° processing

## Summary

# CNFFFT Statistical Analysis

## Configuration

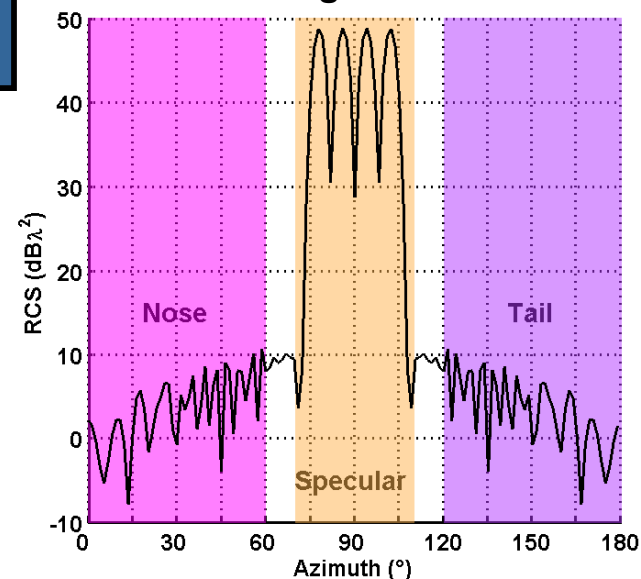
- 4 “wings”; 2 “edges” per wing
- 900 single scatterers per “edge”
- 2 multiple scatterer sets
  - 8 nose-to-tail (N-T)
  - 8 cross-body (X-B)
  - mean RCS (in sm) set equal to single scattering in nose sector
- 2 edge defects
  - placement: 10% from nose/tail
  - size: 3% and 20% of length
  - defect set to produce a 1-2 dB RCS growth in nose sector
- ~7200 total scatterers
- 10 : 4 : 1 (L : W : H) aspect ratio



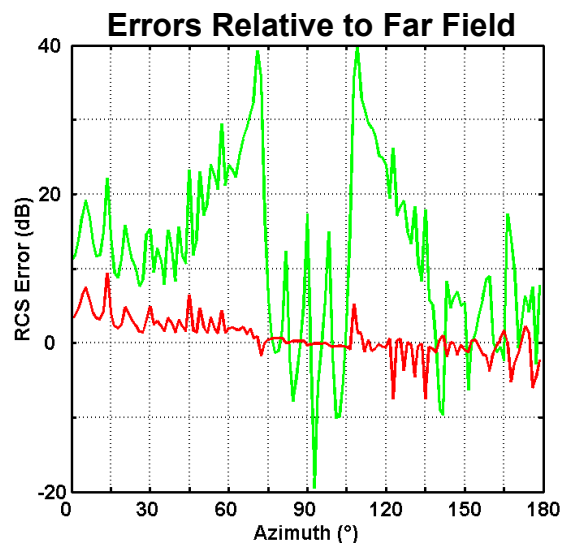
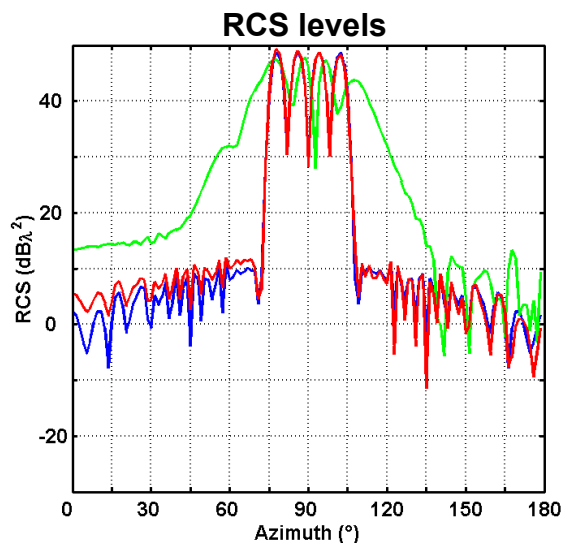
Simulation Parameter	Values
Standoff Distance (T = max target radius)	2.0T, 3.0T, 4.0T
Frequency (target electrical length)	10λ, 30λ, 50λ, 100λ, 300λ

Simulated X-Wing Target

X-Wing Sectors

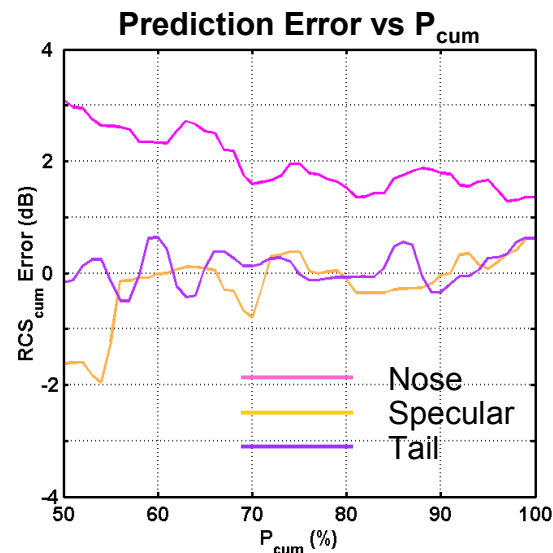
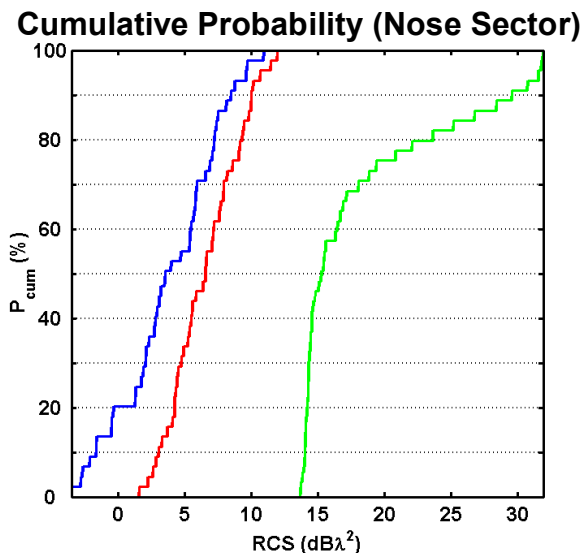


# Example CNFFFT RCS Statistics



**Single Scattering Only**  
 $T = 5\lambda$   
**Standoff = 2.0T**

— Far Field  
 — Near Field  
 — CNFFFT



- CNFFFT significantly reduces point-wise error
  - but error can still at times be non-trivial
- CNFFFT prediction error is instead assessed statistically using RCS  $P_{cum}$  prediction errors within a sector of interest
  - Considering RCS as  $P_{cum}$  distributions is common in RCS diagnostics
- Typical design/manufacturing specifications are defined for  $P_{cum}$  values  $\geq 50\%$



# Outline

## NFFFT Overview

- Background and formulation
- Collection geometries

## → Example CNFFFT Results

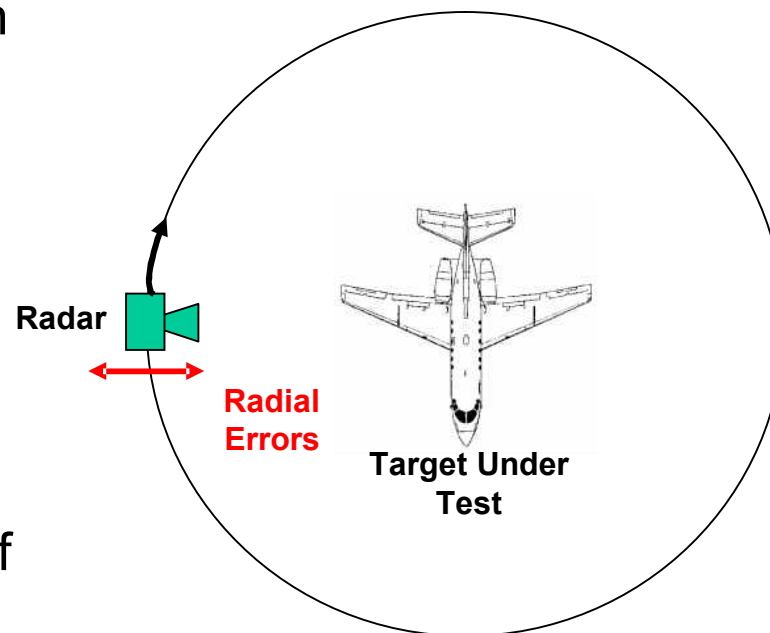
- RCS patterns
- ■ Position error sensitivity
- Antenna pattern compensation
- Sub-360° processing

## Summary

# Position Error Compensation

## Motivation and Approach

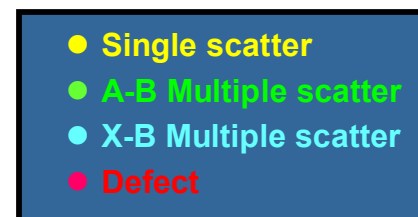
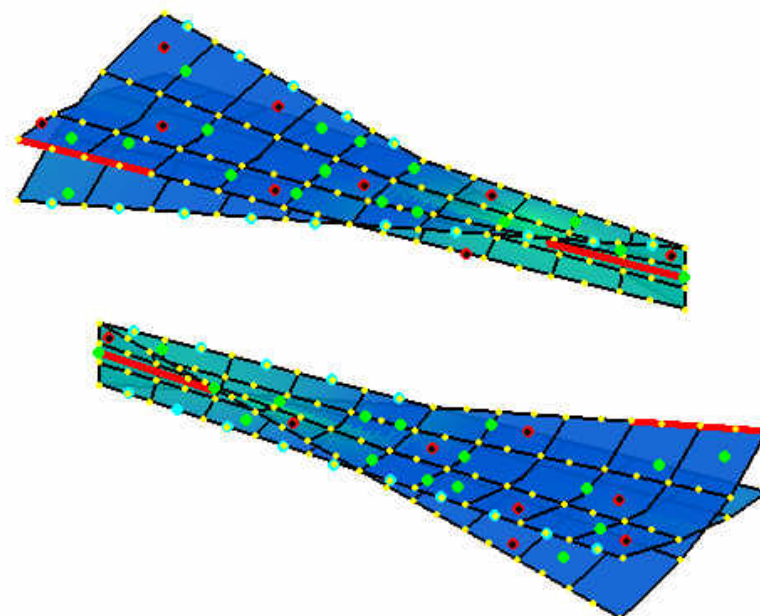
- Evaluate the impact of radial position errors on CNFFT performance
  - ground-based mobile RCS diagnostic systems
  - static NF facilities using string supports
- Assess viability of motion compensation to mitigate error
- Performance is measured in terms of sector RCS  $P_{cum}$  prediction error using simulated data
  - common in RCS diagnostics



# Data Simulations – 1 of 2

## X-Wing Generalized Point Scatterer Target

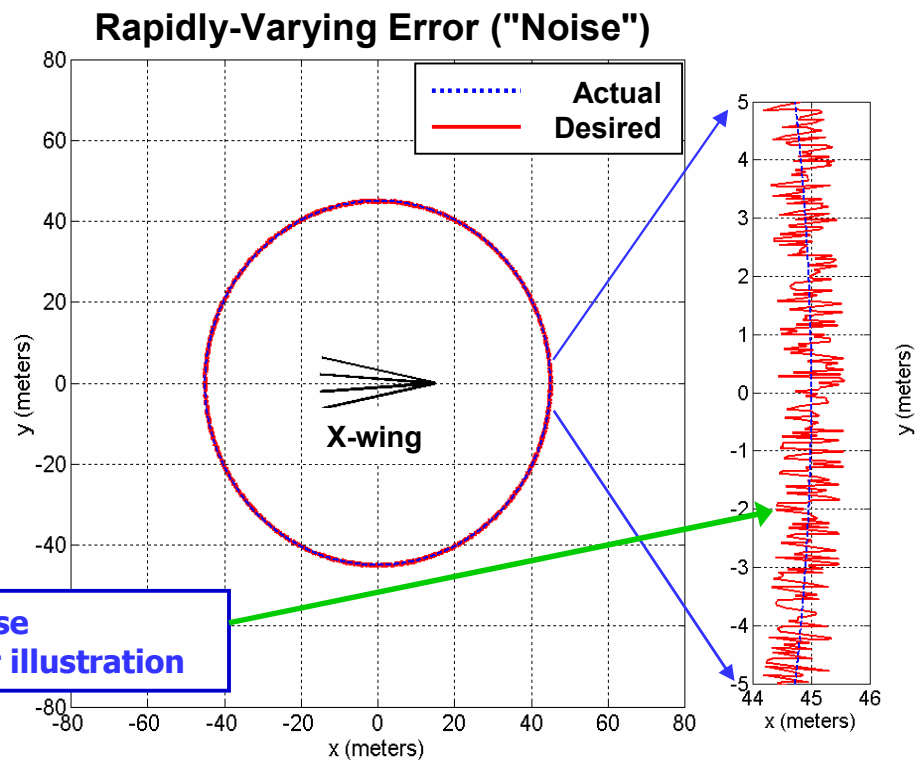
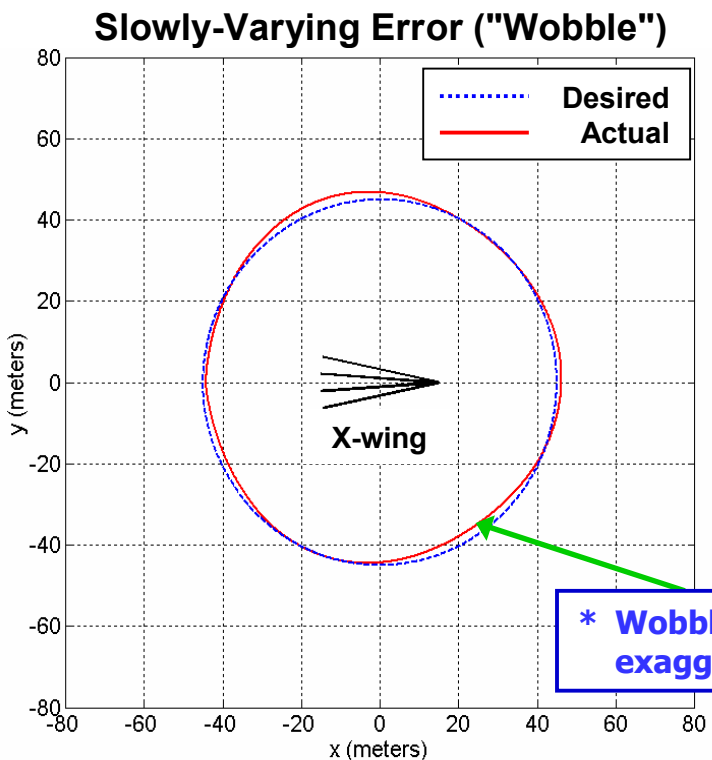
- 4 “wings”; 2 “spokes” per wing
- Dense arrays of single scatterers provide specular flashes from “spokes”
- Multiple scatterer added to produce 1.5 dB RCS growth in nose sector (off-specular “well”)
  - along-body (A-B)
  - cross-body (X-B)
- Single & multiple scatterer “defects” can be switched on & off to produce 1.5 dB RCS growth in nose sector (off-specular “well”)
  - used to simulate damage/repair
  - left “on” for this study
- ~7200 total scatterers
- 10 : 4 : 1 (L : W : H) aspect ratio



Simulation Parameter	Values
Standoff Distance (T = max target radius)	3.0T, 4.8T
<i>Target length at center frequency</i>	<i>300λ</i>

# Data Simulations – 2 of 2

## Simulation Geometries



**\* Wobble and noise exaggerated for illustration**

- Modeled as  $A \cdot (\sin(\theta) + \cos(3.3 \cdot \theta))$ 
  - where  $A$  sets the maximum error level
- Represents drift in position control system
- Modeled as uniformly distributed and over  $[-B, B]$  and uncorrelated angle-to-angle
- Represents vibration in antenna pedestal



# Simulation Error Parameters

## Three Cases Considered

Case	Wobble (A)	Noise (B)
Slowly-Varying Error (Wobble)	$2.0\lambda$	0.0
Rapidly-Varying Error (Mild Noise)	0.0	$0.06\lambda$
Rapidly-Varying Error (Severe Noise)	0.0	$0.2\lambda$

- CNFFFT performance was evaluated with and without a first-order phase compensation

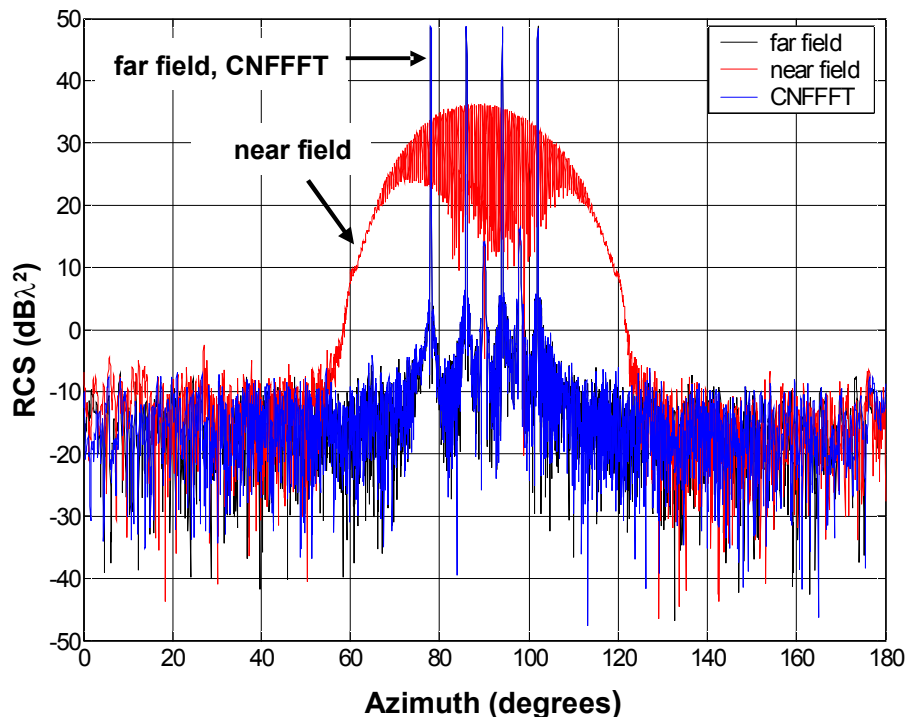
$$S_{comp}^{NF}(\theta) = S^{NF}(\theta)e^{-i2k\Delta r(\theta)}, \quad \Delta r(\theta) = \text{radial offset}$$

- provides perfect compensation at center of measurement circle
- assumes that the radial offset from the ideal circle is known at each aspect angle

# Example CNFFFT Results

## RCS vs Aspect

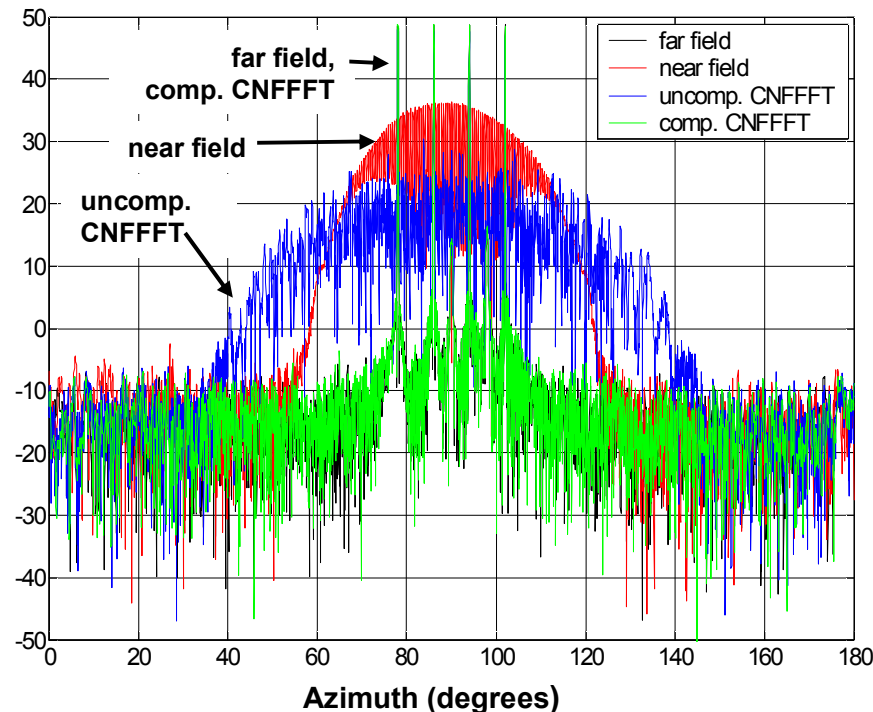
**Error-Free Case**



**Nose Region**    **Specular Region**    **Tail Region**  
 0-60 degrees    75-105 degrees    120-180 degrees

Standoff: 3.0T

**Mild Noise Case**



■ Even small amount of rapidly-varying error can severely degrade CNFFFT performance (w/o compensation)



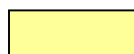
# CNFFFT Prediction Error – 1 of 3

## Unprocessed Near Field Data

NEAR FIELD	Region →	Nose				Tail				Specular			
	Pcum % →	50	80	90	95	50	80	90	95	50	80	90	95
No error	R = 3T	4.3	4.4	4.7	6.0	0.8	1.4	2.2	5.4	34.0	30.4	27.1	19.9
	R = 4.8T	2.0	1.9	1.8	1.7	-0.4	-0.3	-0.3	-0.2	34.5	30.5	26.9	19.4
Slowly-varying error	R = 3T	4.4	4.4	4.8	6.1	0.9	1.4	2.2	5.3	34.0	30.4	27.1	19.9
	R = 4.8T	2.0	1.9	1.8	1.7	-0.4	-0.3	-0.2	-0.2	34.5	30.5	26.9	19.4
Rapidly-varying error: mild	R = 3T	4.3	4.4	4.7	6.0	0.8	1.4	2.2	5.5	34.0	30.4	27.1	19.9
	R = 4.8T	2.0	1.9	1.8	1.7	-0.4	-0.3	-0.3	-0.2	34.5	30.5	26.9	19.4
Rapidly-varying error: severe	R = 3T	4.3	4.4	4.7	6.0	0.8	1.4	2.2	5.5	34.0	30.4	27.1	19.9
	R = 4.8T	2.0	1.9	1.8	1.7	-0.4	-0.3	-0.3	-0.2	34.5	30.5	26.9	19.4



Error ≤ 1 dB



1 dB < Error ≤ 2 dB



Error > 2 dB

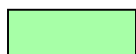
- Near field (unprocessed) RCS error is greatest in specular region
- Near field (unprocessed) RCS error is relatively insensitive to position errors
  - errors affect primarily the near field phase



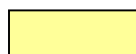
# CNFFFT Prediction Error – 2 of 3

## Uncompensated CNFFFT

UNCOMPENSATED CNFFFT	Region →	Nose				Tail				Specular			
	Pcum % →	50	80	90	95	50	80	90	95	50	80	90	95
No error	R = 3T	0.9	0.9	0.8	0.8	0.0	0.0	0.0	0.0	0.3	0.3	0.3	0.3
	R = 4.8T	0.5	0.5	0.5	0.5	-0.1	0.0	0.0	-0.1	0.1	0.1	0.2	0.0
Slowly-varying error	R = 3T	0.9	0.9	0.9	0.9	0.0	0.0	0.0	0.0	2.4	10.5	25.1	24.7
	R = 4.8T	0.5	0.5	0.5	0.5	-0.1	-0.1	-0.1	-0.1	0.9	1.9	8.9	18.6
Rapidly-varying error: mild	R = 3T	5.6	17.5	22.4	24.3	5.1	17.7	21.5	23.4	22.4	20.1	17.6	11.7
	R = 4.8T	2.2	3.4	7.7	13.2	1.9	3.1	8.7	14.7	23.6	21.2	18.8	12.9
Rapidly-varying error: severe	R = 3T	8.3	24.4	29.0	31.0	7.7	24.7	28.3	30.2	28.9	26.3	23.4	16.7
	R = 4.8T	4.1	6.0	13.9	20.8	3.4	5.7	14.9	22.0	30.1	27.4	24.6	17.9



Error ≤ 1 dB



1 dB < Error ≤ 2 dB



Error > 2 dB

- Uncompensated CNFFFT is extremely sensitive to rapidly-varying position errors
- Sensitivity to slowly-varying errors is limited to the specular region
  - although all regions show improvement relative to unprocessed near field data



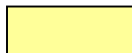
# CNFFFT Prediction Error – 3 of 3

## Compensated CNFFFT

COMPENSATED CNFFFT	Region →	Nose				Tail				Specular			
	Pcum % →	50	80	90	95	50	80	90	95	50	80	90	95
No error	R = 3T	0.9	0.9	0.8	0.8	0.0	0.0	0.0	0.0	0.3	0.3	0.3	0.3
	R = 4.8T	0.5	0.5	0.5	0.5	-0.1	0.0	0.0	-0.1	0.1	0.1	0.2	0.0
Slowly-varying error	R = 3T	0.9	0.9	0.8	0.8	0.0	0.0	0.0	0.2	0.6	1.2	6.0	9.9
	R = 4.8T	0.5	0.5	0.5	0.4	-0.1	0.0	0.0	0.0	0.3	0.3	2.9	1.1
Rapidly-varying error: mild	R = 3T	0.9	1.0	0.9	0.9	0.0	0.1	0.1	0.1	0.4	0.3	0.3	0.0
	R = 4.8T	0.5	0.5	0.5	0.5	-0.1	0.0	0.0	-0.1	0.2	0.1	0.2	0.0
Rapidly-varying error: severe	R = 3T	1.3	1.4	1.4	1.4	0.5	0.7	0.8	0.8	1.0	0.5	0.6	0.0
	R = 4.8T	0.5	0.5	0.5	0.5	0.0	0.0	0.0	0.0	0.3	0.1	0.2	0.0



Error ≤ 1 dB



1 dB < Error ≤ 2 dB



Error > 2 dB

- Compensated CNFFFT performance is very good over all sectors for all three error cases
  - exception is specular region for slowly-varying errors



# Outline

## NFFFT Overview

- Background and formulation
- Collection geometries

## → Example CNFFFT Results

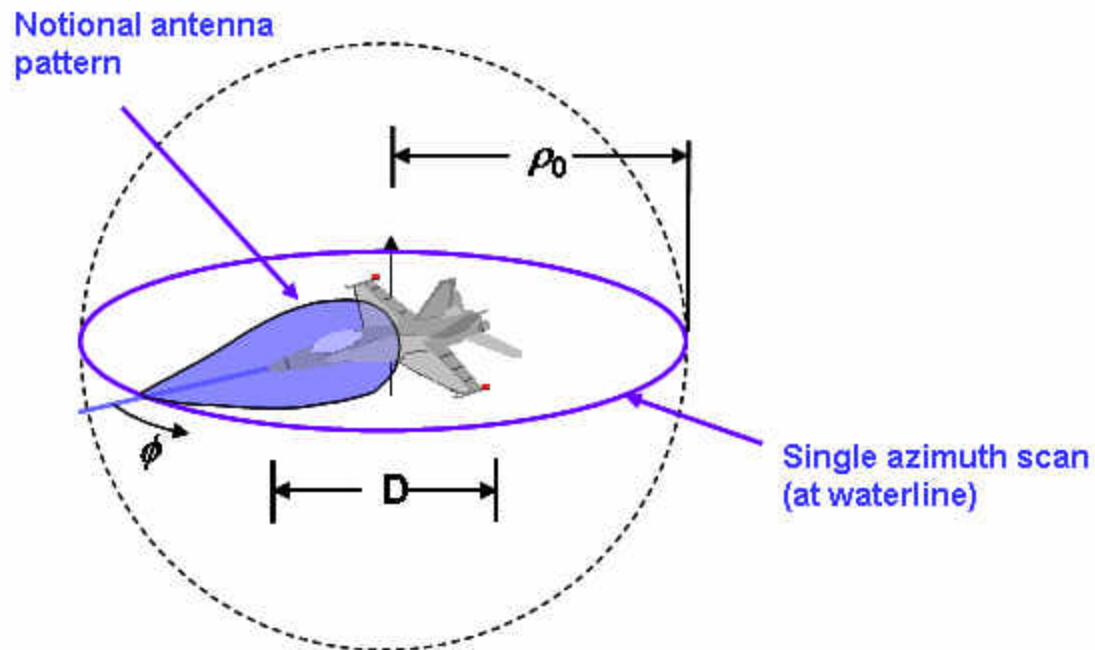
- RCS patterns
- Position error sensitivity
- ■ Antenna pattern compensation
- Sub-360° processing

## Summary

# CNFFFT Antenna Pattern Compensation

## Assumptions

- Target is in the far field of the antenna
  - but antenna is still in the near field of the target
- Amplitude (and phase) of far-field antenna pattern are known (in waterline plane)
  - one-way or two-way
- Antenna is boresighted on the center of rotation





# CNFFFT APC Implementation Summary\*

$$U'(\phi, k) = \frac{1}{\pi \sqrt{\rho_0}} \int R_0^{3/2} e^{i2kR_0} \int u(\phi, k') e^{-i2k'R_0} dk' dR_0$$

Implemented with a pair of FFTs in the frequency domain

$$S_{FF}(\phi, k) = 2 \sqrt{\frac{\rho_0}{i\pi k}} \sum_{n=-N}^N \frac{(-i)^n e^{in\phi}}{P_n(2k\rho_0)} \int_0^{2\pi} U'(\phi_0, k) e^{-in\phi_0} d\phi_0$$

Implemented with a pair of FFTs in the angle domain

This is the only difference relative to the CNFFFT w/o APC

— where

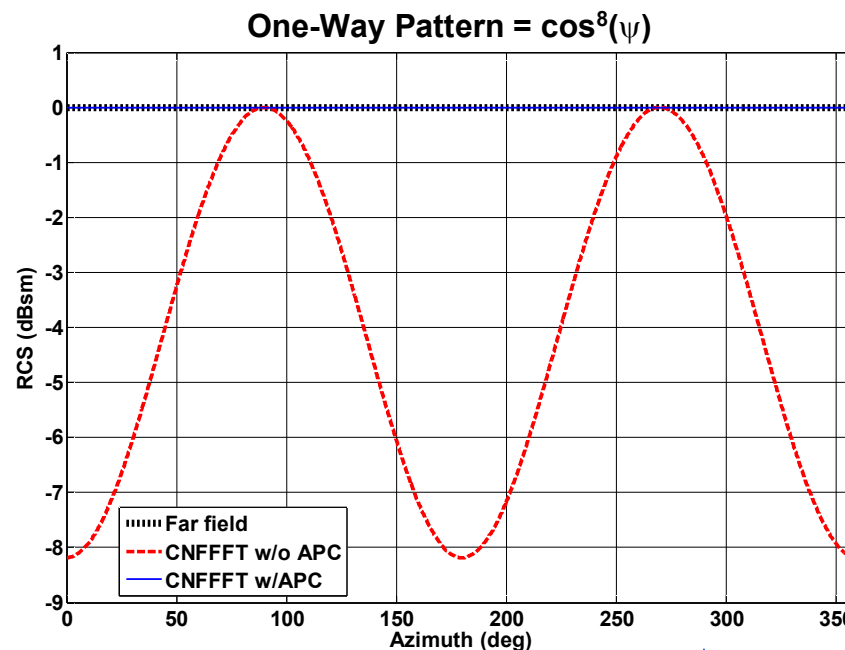
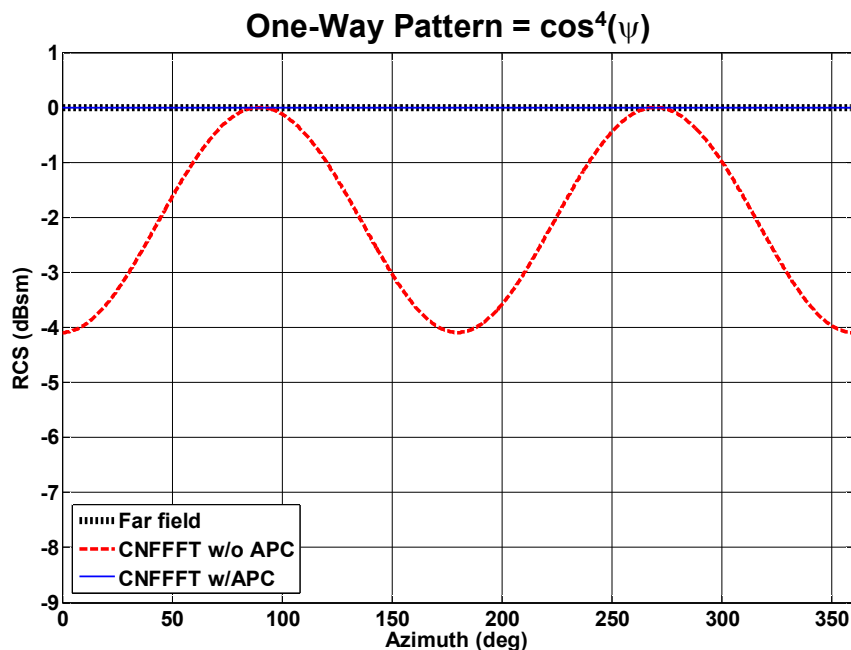
$$P_n(2k\rho_0) = \sum_{m=-M}^M i^m a_m H_{n+m}^{(1)}(2k\rho_0)$$

$a_m$  = antenna pattern Fourier coefficients

\* Coleman, C. et. al. (2005), "Antenna Pattern Correction for the Circular Near Field-to-Far Field Transformation (CNFFFT)," *Proc. AMTA '05*, pp. 202-207.

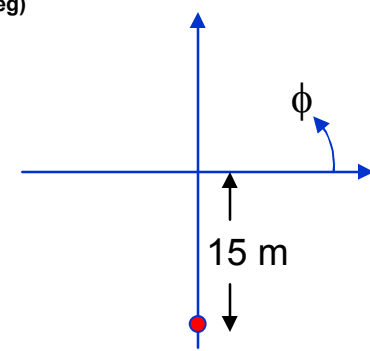
# CNFFFT with APC Performance – 1 of 4

## RCS Vs Azimuth (3 GHz)



- CNFFFT with APC reduces pattern errors to essentially zero

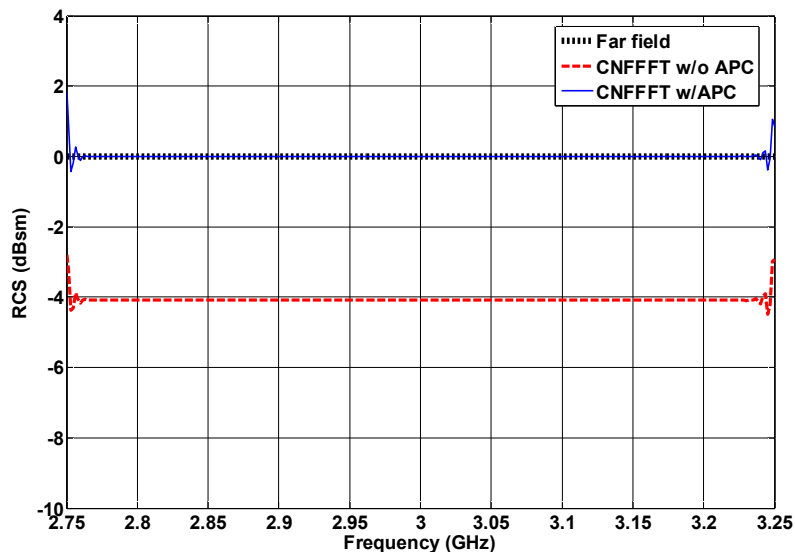
Single point scatterer  
 Freq band: 2.75 - 3.25 GHz  
 Measurement radius: 45 m



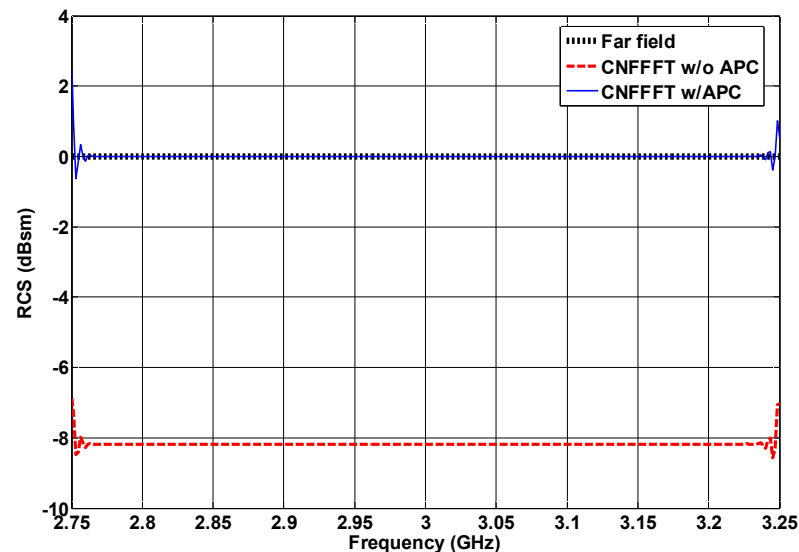
# CNFFFT with APC Performance – 2 of 4

## RCS Vs Frequency (Azimuth = 0°)

One-Way Pattern =  $\cos^4(\psi)$

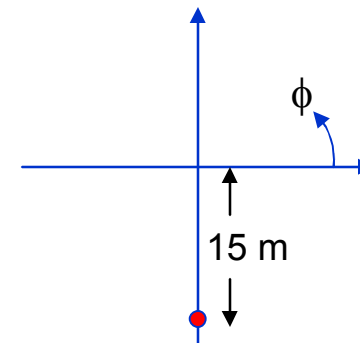


One-Way Pattern =  $\cos^8(\psi)$



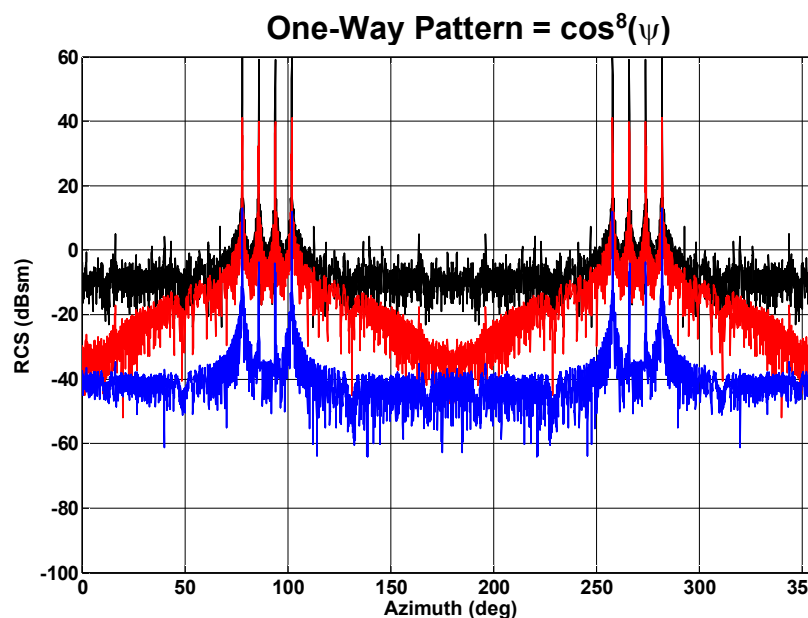
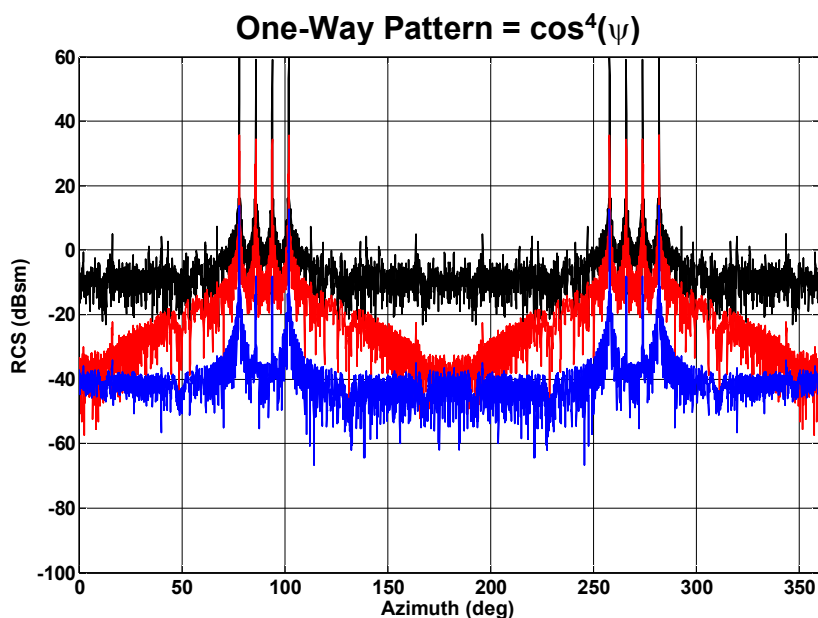
- APC is excellent across the entire band
  - neglecting band edge effects

Single point scatterer  
 Freq band: 2.75 - 3.25 GHz  
 Measurement radius: 45 m

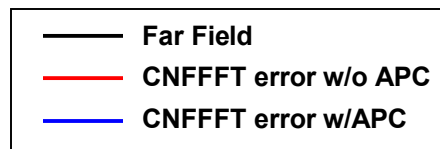


# CNFFFT with APC Performance – 3 of 4

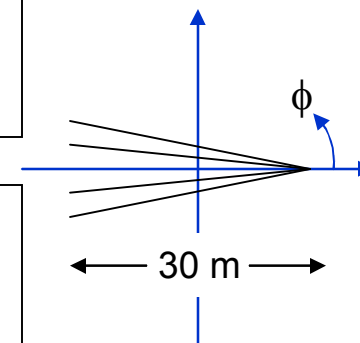
## RCS Error Vs Azimuth (3 GHz)



- Pattern errors are most significant near broadside
- Residual error after APC is primarily due to out-of-plane NF effects

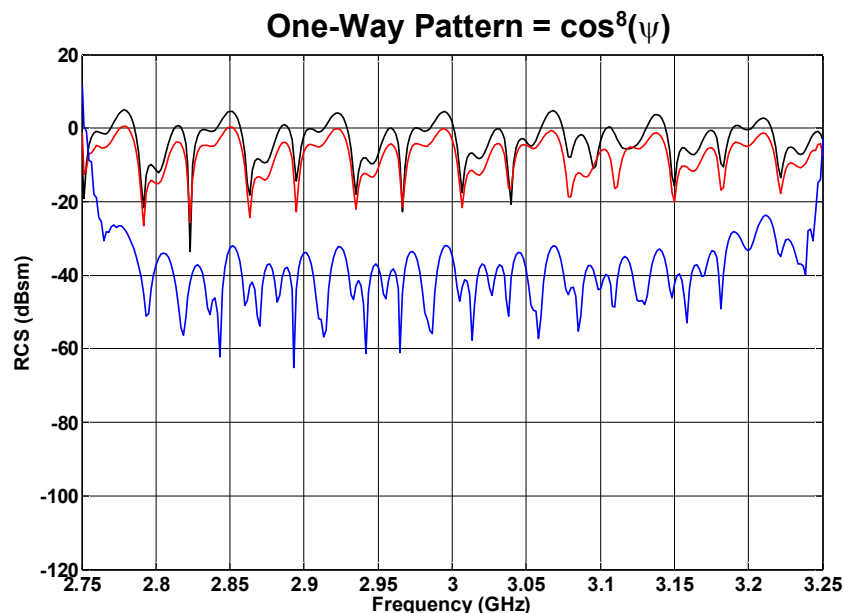
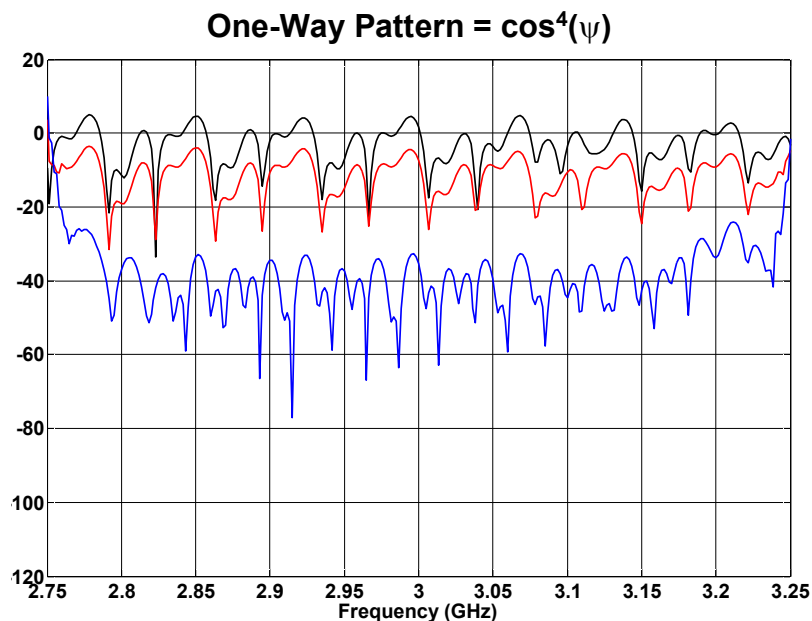


X-wing target  
 Freq band: 2.75 - 3.25 GHz  
 Measurement radius: 45 m

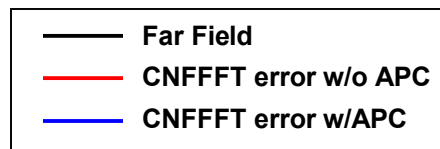


# CNFFFT with APC Performance – 4 of 4

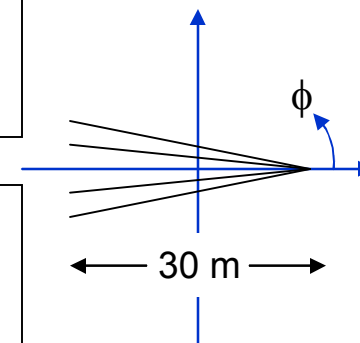
## RCS Error Vs Frequency (Azimuth = 90°)



- APC is excellent across the entire band
  - neglecting band edge effects



**X-wing target**  
 Freq band: 2.75 - 3.25 GHz  
 Measurement radius: 45 m





# Outline

## NFFFT Overview

- Background and formulation
- Collection geometries

## → Example CNFFFT Results

- RCS statistics
- Position error sensitivity
- Antenna pattern compensation
- ■ Sub-360° processing

## Summary

# 360° CNFFFT Formulation

- Note that the CNFFFT can be discretized and implemented as a pair of appropriately weighted angular FFTs
  - Recall CNFFFT formulation for an isotropic antenna:

Far field scattering pattern estimate  $S_{FF}(\phi, k)$  computed from preprocessed near field  $U'(\phi, k)$ :

$$S_{FF}(\phi, k) = 4\pi \sqrt{\frac{\rho_c}{i\pi k}} \sum_{n=-N}^N \frac{(-i)^n e^{in\phi}}{H_n^{(1)}(2k\rho_c)} \frac{1}{2\pi} \int_0^{2\pi} U'(\phi, k) e^{-in\phi} d\phi$$

This summation is DFT #2

Once discretized, this integral becomes DFT #1

- For a non-isotropic antenna, the Hankel functions are replaced by a set of probe compensation factors as discussed previously
  - but the CNFFFT is still computed using a pair of DFT's



# Sub-360° CNFFFT Formulation – 1 of 2

- Define the  $n^{\text{th}}$  azimuthal harmonic of the preprocessed near-field (NF) data at wavenumber  $k$ :

$$U'_n(k) = \frac{1}{2\pi} \int_0^{2\pi} U'(\phi, k) e^{-in\phi} d\phi$$

- Define the  $n^{\text{th}}$  azimuthal harmonic of the far-field (FF) data at wavenumber  $k$ :

$$S_{n,FF}(k) = 2\pi \left[ 2\sqrt{\frac{\rho_c}{i\pi k}} \frac{(-i)^n}{H_n^{(1)}(2k\rho_c)} \right] U'_n(k)$$

— note that the far-field harmonics are the product of the sequence in brackets and the modified near-field harmonics

- The inverse DFT of the above sequence in brackets thus defines a convolution kernel in the azimuth domain
  - yields far-field data when convolved with the modified near-field data (and scaled by  $2\pi$ )

# Sub-360° CNFFFT Formulation – 2 of 2

## CNFFFT Equation in Azimuthal Harmonic Domain

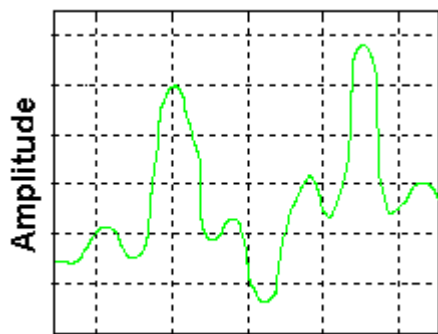
$$S_{n,FF}(k) = 2\pi \left[ 2\sqrt{\frac{\rho_c}{i\pi k}} \frac{(-i)^n}{H_n^{(1)}(2k\rho_c)} \right] U'_n(k)$$

DFT/  
IDFT

DFT/  
IDFT

DFT/  
IDFT

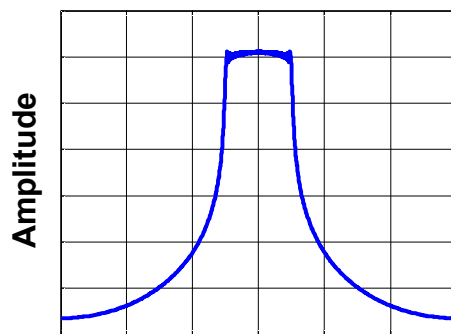
Far Field



Azimuth

=

CNFFFT Kernel

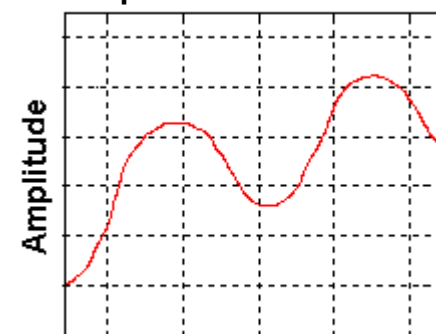


Azimuth

\*

convolution

Preprocessed Near Field



Azimuth

Since the CNFFFT kernel has a finite width in azimuth (to a very good approximation), we can determine *a priori* how much NF data must be collected to support a given FF angular sector

# CNFFFT Convolution Kernel Parameterization

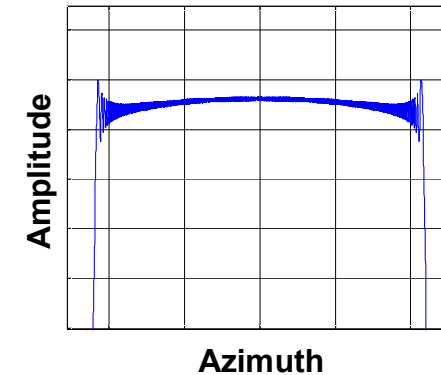
## CNFFFT Equation

$$S_{n,FF}(k) = 2\pi \left[ 2\sqrt{\frac{\rho_c}{i\pi k}} \frac{(-i)^n}{H_n^{(1)}(2k\rho_c)} \right] U'_n(k)$$

IDFT

DFT

## CNFFFT Kernel



Kernel is a function of two parameters:

- Lumped parameter  $2k\rho_c$
- Number of azimuthal harmonics  $2N+1$  computed
  - $N$  is selected to capture all significant target azimuthal harmonics\*
  - $N = 2k\rho_t + n_1$
  - $n_1$  is relatively small compared to  $2k\rho_t$  (typically 3 orders of magnitude smaller)

\*(Jensen, F. and Frandsen, A., *Proc. AMTA '04*)

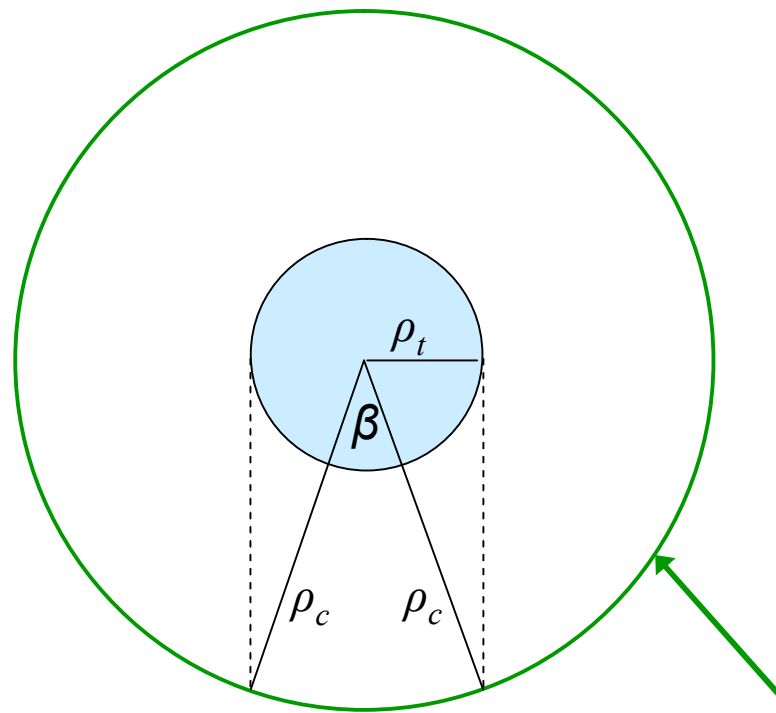
These parameters can be expressed in terms of two other (normalized) parameters:

- Maximum target radius in wavelengths ( $\rho_t / \lambda$ )
- Standoff distance relative to maximum target radii ( $\rho_c / \rho_t$ )

$$2k\rho_c = (4\pi/\lambda)(\rho_c/\rho_t)\rho_t = (4\pi)(\rho_c/\rho_t)(\rho_t/\lambda)$$

$$N = 2k\rho_t + n_1 = (4\pi)(\rho_t/\lambda) + n_1$$

# Geometric Approximation of CNFFFT Kernel Width



- Project the target's maximum radius circle onto the measurement circle
- The angle  $\beta$  subtended by this projection is approximately equal to the width of the CNFFFT kernel
- Next slide illustrates accuracy of approximation

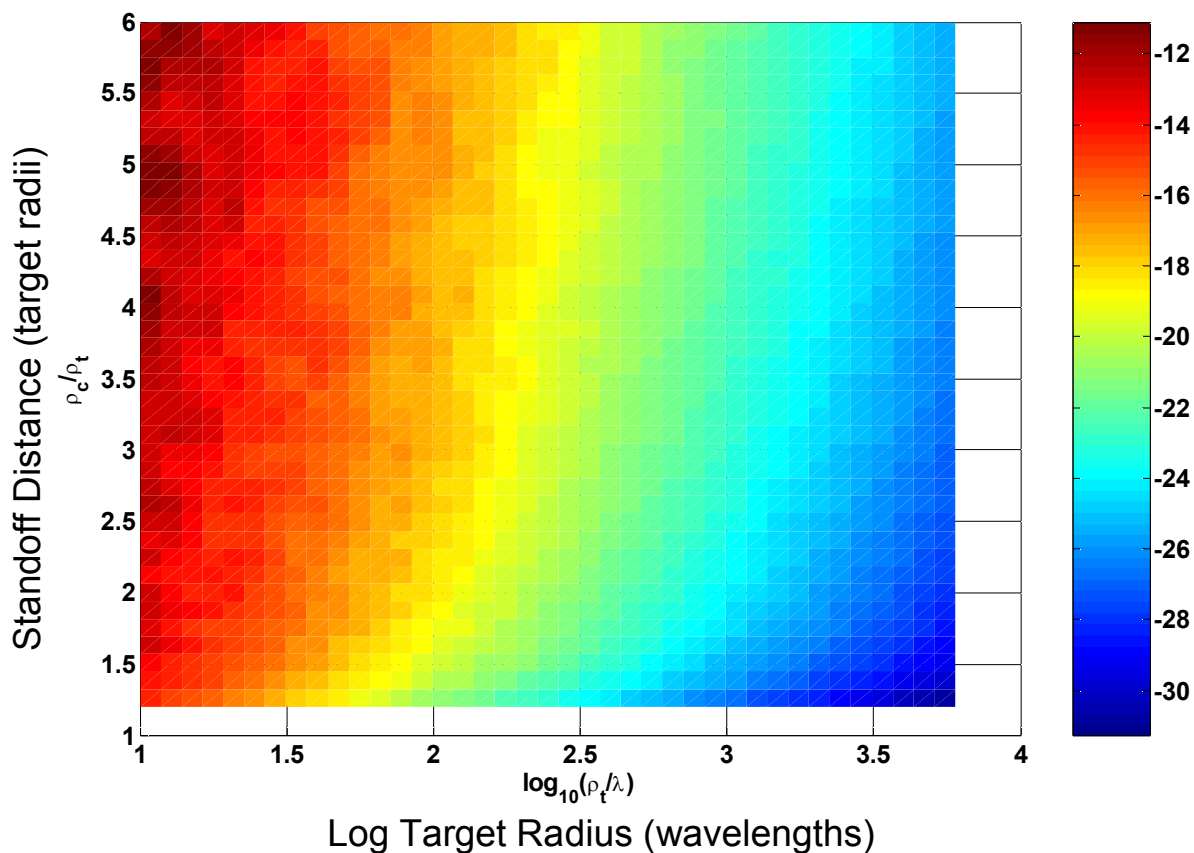
Measurement Circle

$$\beta = 2 \sin^{-1}(\rho_t / \rho_c)$$



# Accuracy of Geometric Approximation

Truncated Kernel Energy Relative to the Total CNFFFT Kernel Energy (dB)

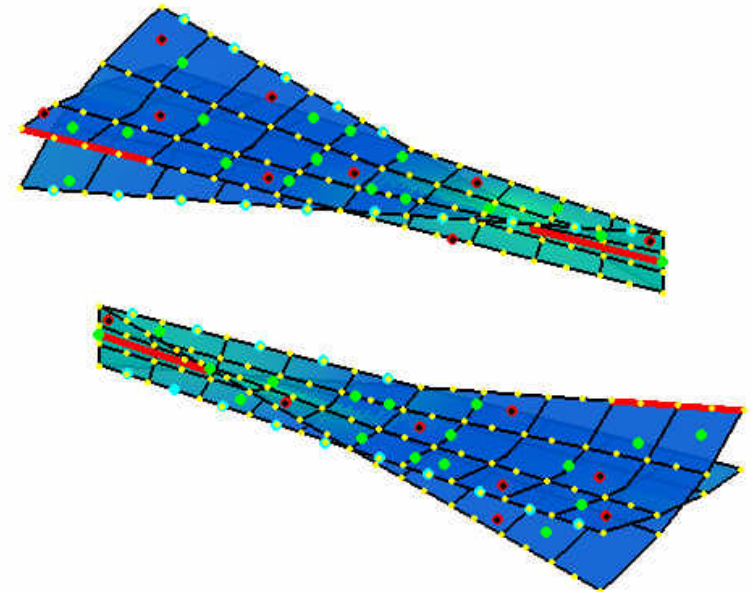


The geometrical approximation is a reasonable “first cut” to estimate the CNFFFT kernel width, especially for higher  $\rho_t/\lambda$  values

# Sub-360° CNFFFT Numerical Tests

## X-Wing Generalized Point Scatterer Target

- 4 “wings”; 2 “spokes” per wing
- Dense arrays of single scatterers provide specular flashes from “spokes”
  - scatterer spacing determined by simulation frequency to avoid grating lobes
- 10 : 4 : 1 (L : W : H) aspect ratio
- X-wing target can include multi-bounce scatterers and defects which violate the assumptions upon which the CNFFFT is based
  - these were set to zero because we are only concerned with demonstrating relative error between the full-360° and sub-360° CNFFFTs



- Single scatterer
- Along-body multiple scatterer
- Cross-body multiple scatterer
- Defect

# Simulation Geometry and Parameters

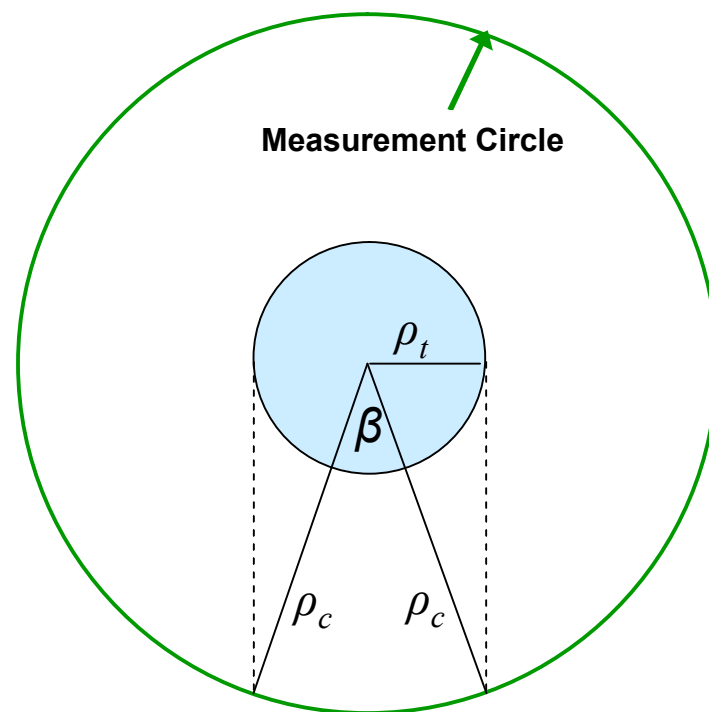
## Two Frequency Bands

	Low Band	High Band
Standoff Distance ( $\rho_c$ )	$3\rho_t$	
Geometric Kernel Width ( $\beta$ )	$38.9^\circ$	
Max Target Radius ( $\rho_t$ )	$150\lambda$	$750\lambda$
Fractional Bandwidth	16.7%	1.67%
Frequency Sample Spacing	for unaliased range interval = $4\rho_t$	
Azimuth Sample Spacing	1.5X Nyquist*	

\*Based on two-way -50 dB truncation of near-field azimuthal harmonics (Jensen, F. and Frandsen, A., *Proc. AMTA '04*)

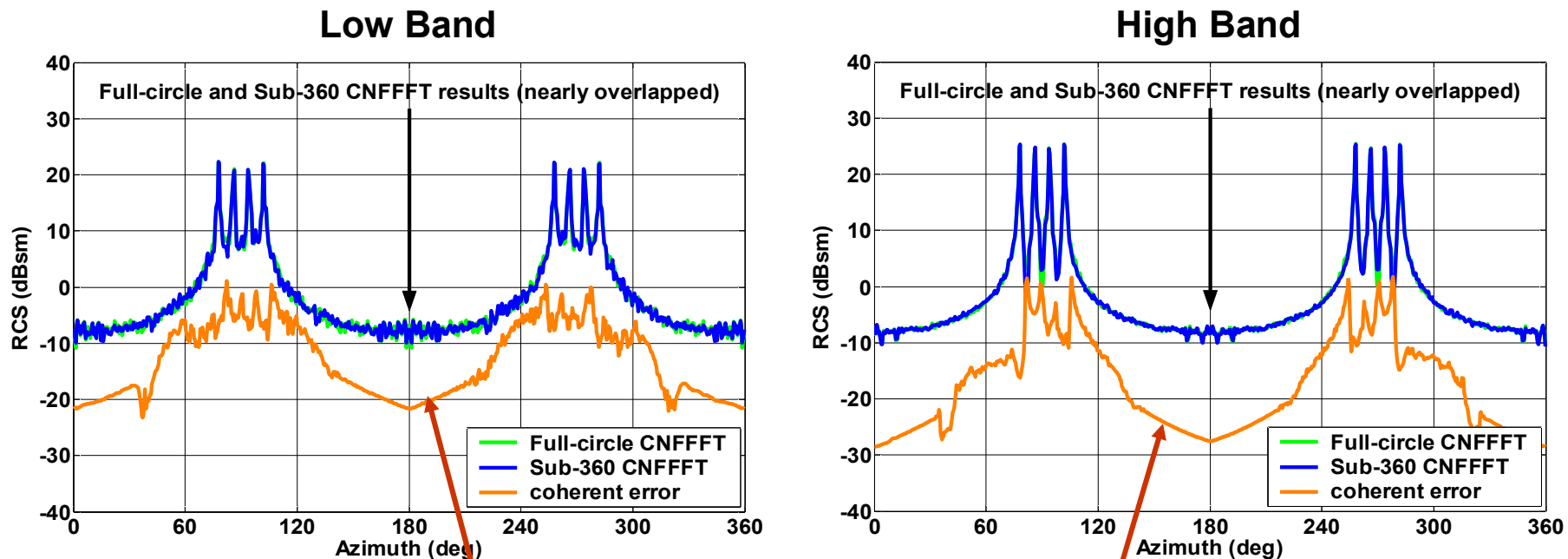
- NF data were simulated over a full-360°
- NF data were processed with both the full-360° and sub-360° CNFFFTs
  - sub-360° CNFFFT can be applied to any collection larger than the kernel width
- The results were evaluated in terms of coherent residual error for various truncated kernel widths

$$\text{coherent error} = \left| S_{FF}^{full\ 360} - S_{FF}^{sub\ 360} \right|^2$$



# Example Coherent Error Plot: 45°-Wide Kernel

## RCS Versus Azimuth (1° medianized plots)

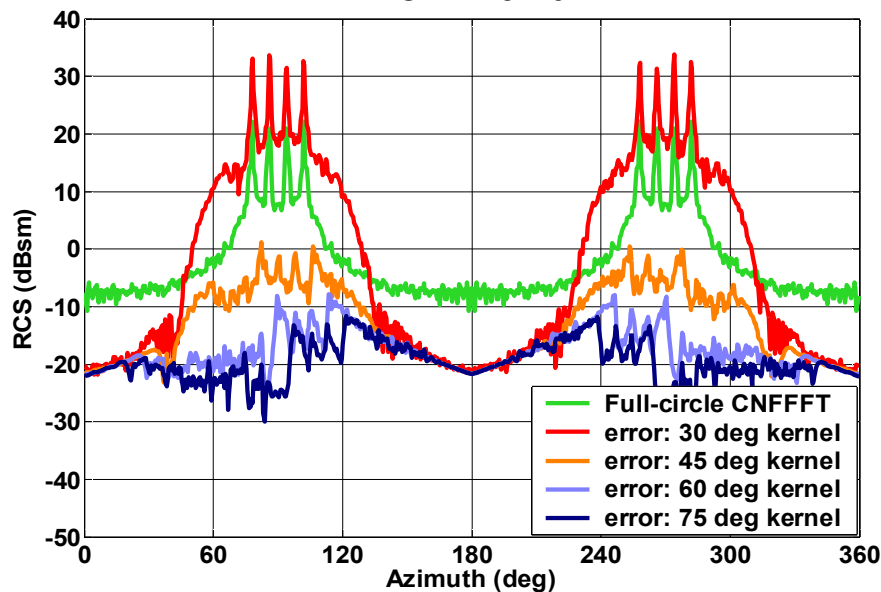


**The coherent error metric allows us to better see the differences between the overlapping full-360° and sub-360° CNFFFT predictions**

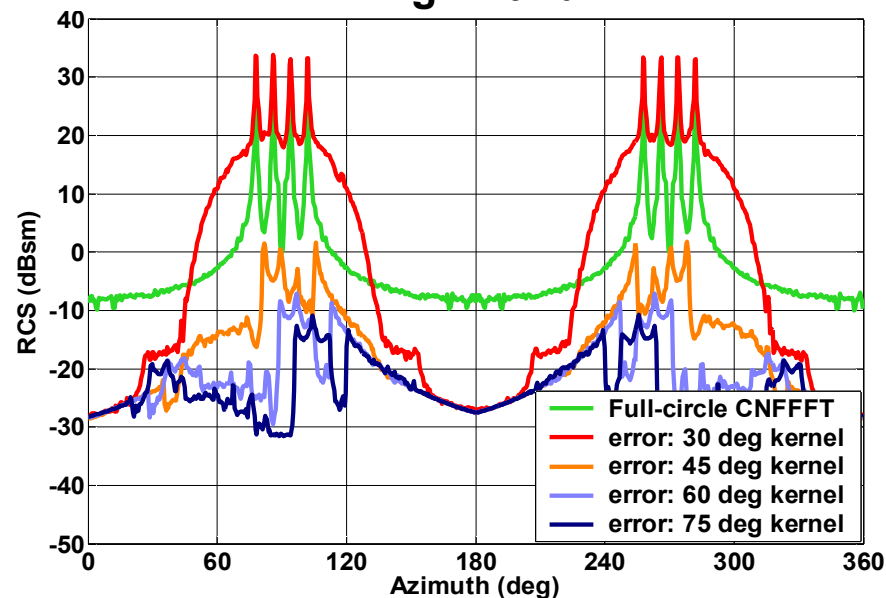
# Sub-360° CNFFFT Error Versus Kernel Width

## RCS Versus Azimuth (1° medianized plots)

### Low Band



### High Band



- For a 30° kernel, the results are unacceptable
- For a 45° kernel, the residual error is typically 10dB below the full-360° CNFFFT
- For the 60° and 75° kernels, the residuals error is typically 12-18 dB below the full-360° CNFFFT

**From the above (and additional observations), a kernel width about 15% greater than the geometric kernel width  $\beta$  (38.9° for this case) will produce respectable sub-360° CNFFFT results**



# Outline

## NFFFT Overview

- Background and formulation
- Collection geometries

## Example CNFFFT Results

- RCS patterns
- RCS statistics
- Position error sensitivity
- Antenna pattern compensation
- Sub-360° processing

## Summary



# Image-Based NFFFT Summary

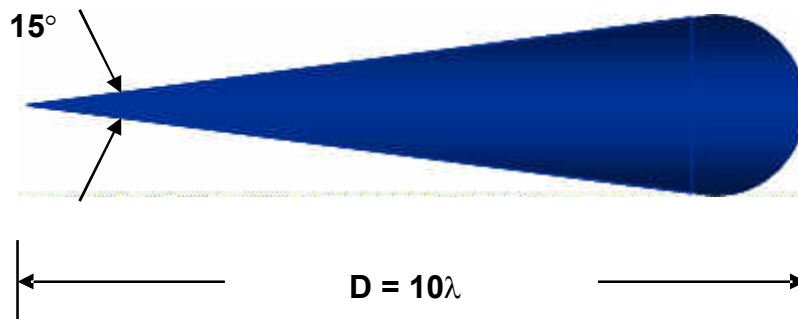
- The IB-NFFFT has been shown to provide robust and accurate far field predictions for a wide range of targets, frequencies, and collection geometries
  - both RCS patterns and sector statistics
- The algorithm has been formulated for many of the common measurement geometries
  - 2-D scans: spherical, planar
    - extension to cylindrical is straightforward
  - 1-D scans: circular and sub-circular, linear
- In this presentation, we have focused on the IB-NFFFT formulation for circular and sub-circular measurement geometries.
- Methods for mitigating IB-NFFFT measurement errors have been developed
  - position errors: circular
  - antenna pattern: circular & linear
  - extensions to other scan geometries are planned
- IB-NFFFT algorithms have been demonstrated and/or implemented on operational systems with our customers
  - both indoor and outdoor measurement facilities



# Appendix 1: CNFFFT with MoM and measured data

# CNFFFT Example - MoM Simulations – 1 of 2

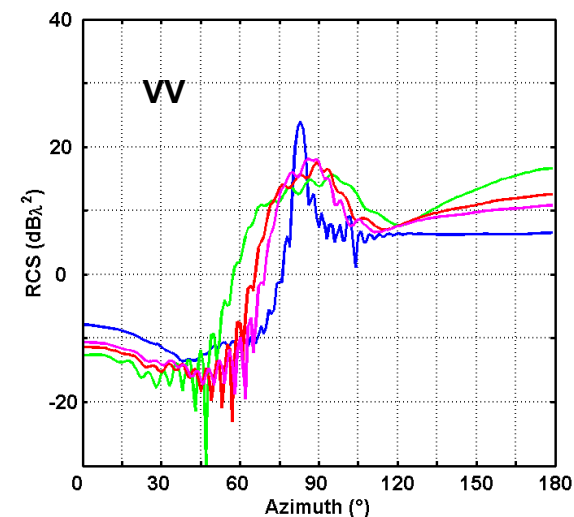
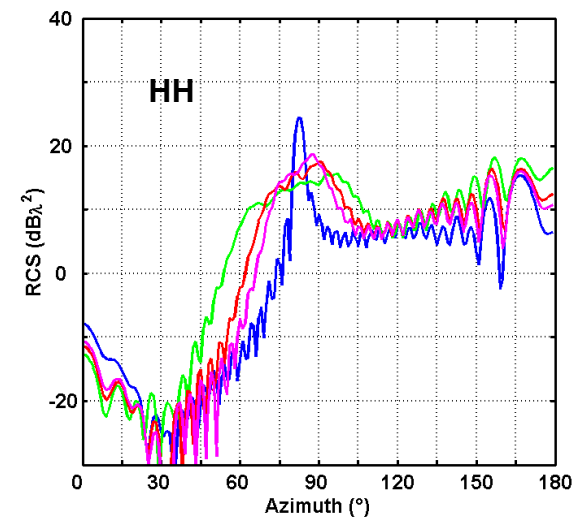
**Conesphere Target**



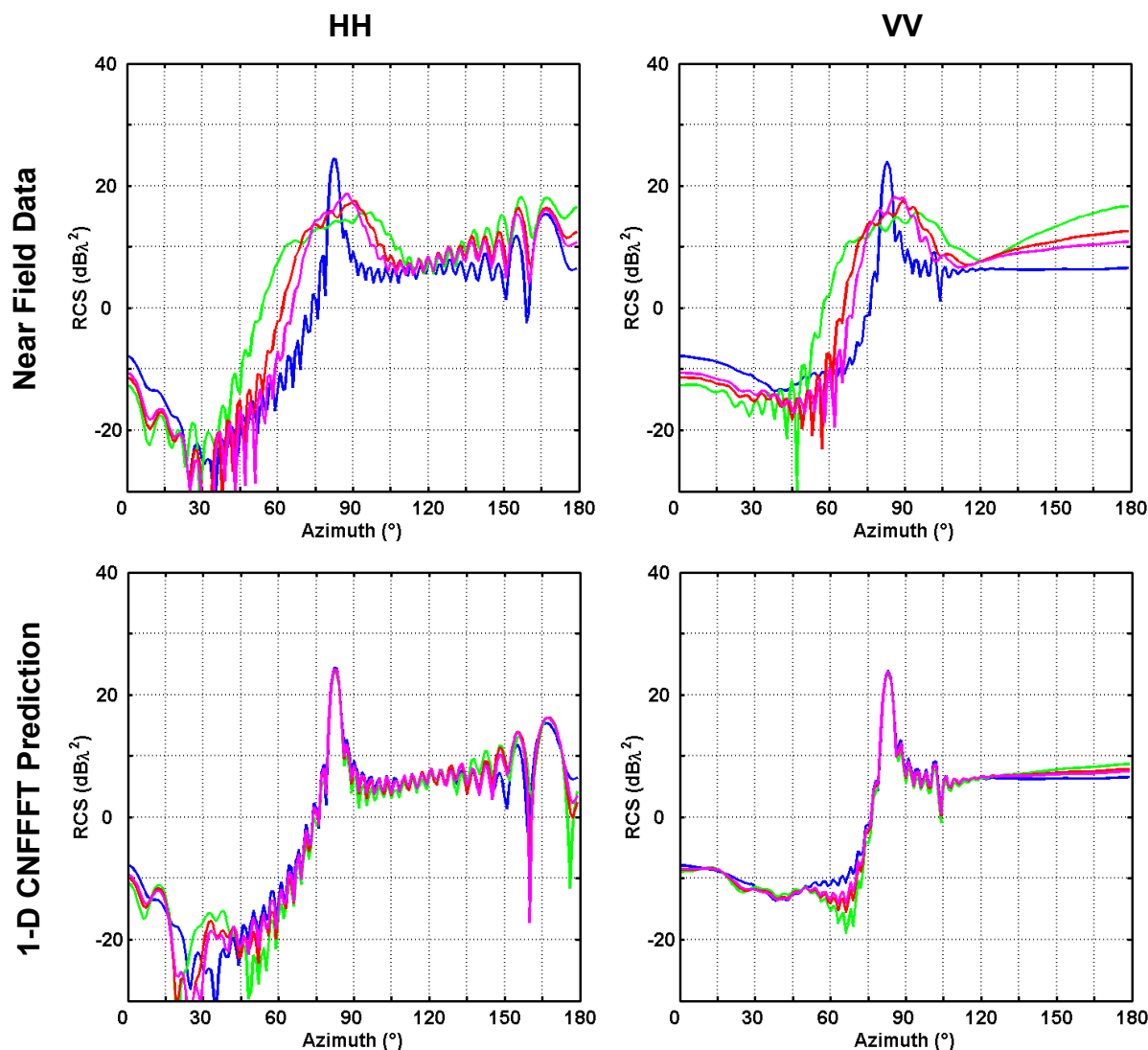
- NF data differ significantly from far field throughout entire pattern

— Far Field  
— NF (R = 1.0D)  
— NF (R = 1.5D)  
— NF (R = 2.0D)

**Simulated Near Field Data**



# CNFFFT Example - MoM Simulations – 2 of 2



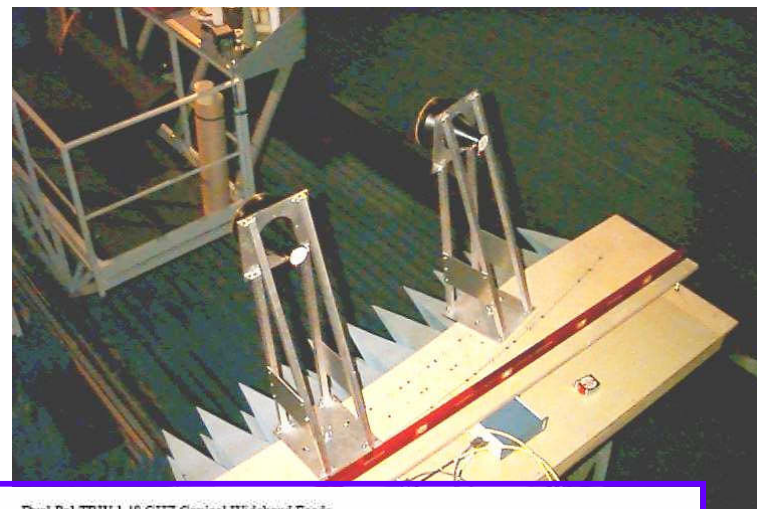
**Conesphere Target  
RCS Versus Azimuth  
D = 10λ**

— Far Field  
— NF (R = 1.0D)  
— NF (R = 1.5D)  
— NF (R = 2.0D)

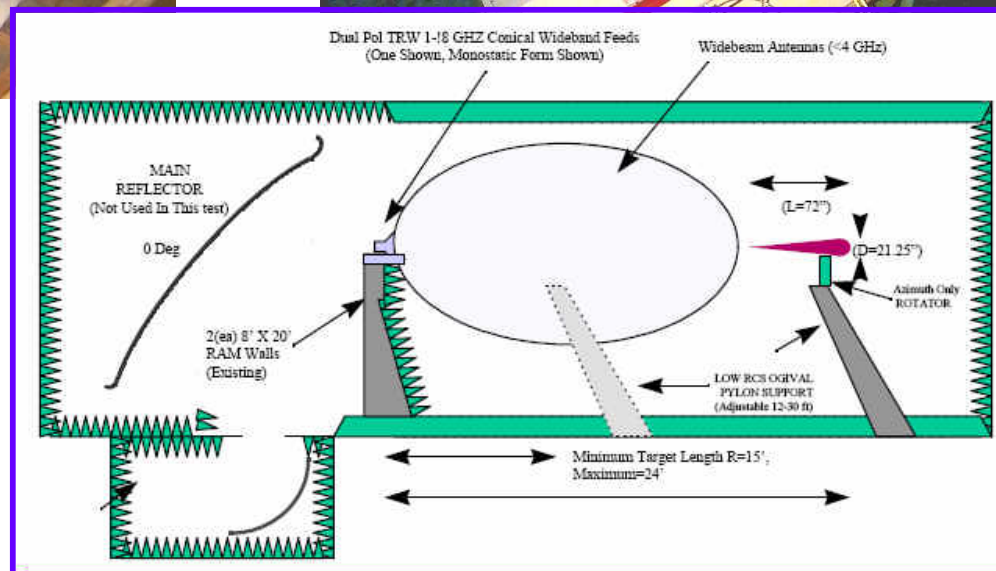
- NFFFT has substantially improved agreement with FF RCS
  - especially at VV pol

# CNFFFT Example – Measured Data – 1 of 3

## AFRL ACR Measurements



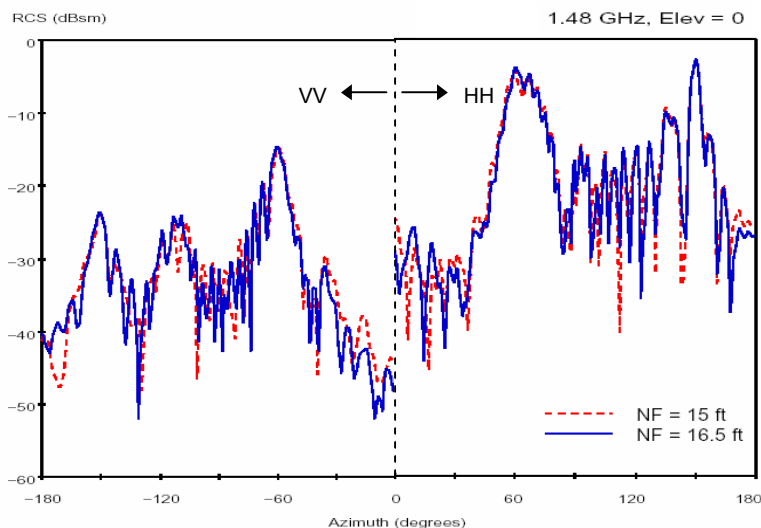
**AFRL "Delta Dart" (D2) test body**  
**Circular (1-D) near field data**



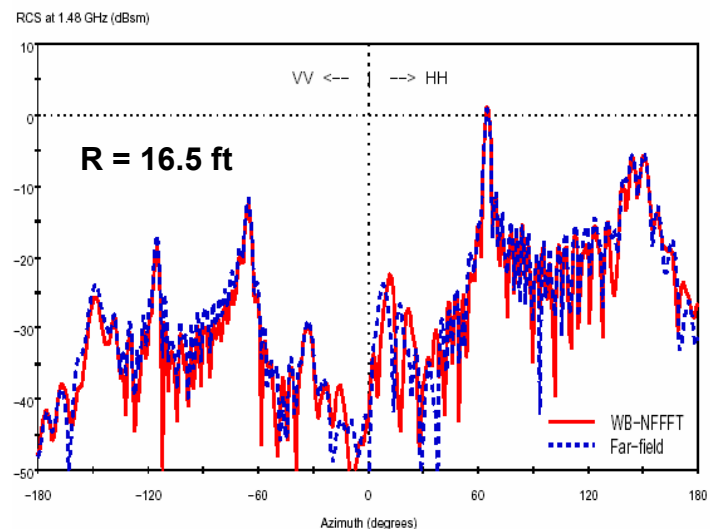
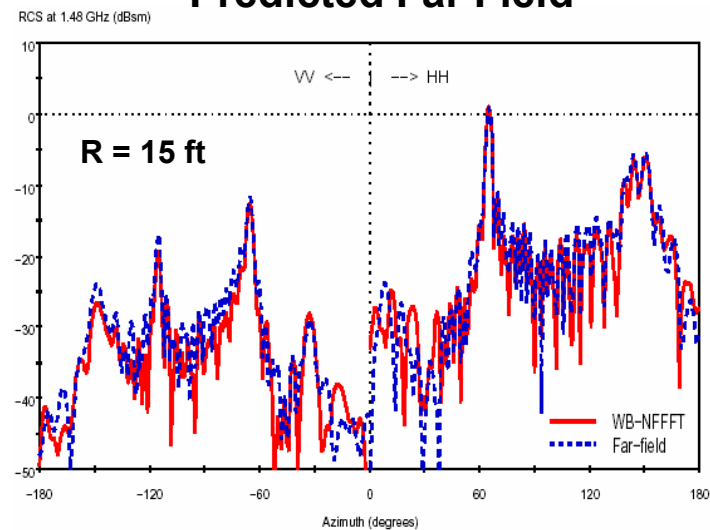


# CNFFFT Example – Measured Data – 2 of 3

## Measured Near Field



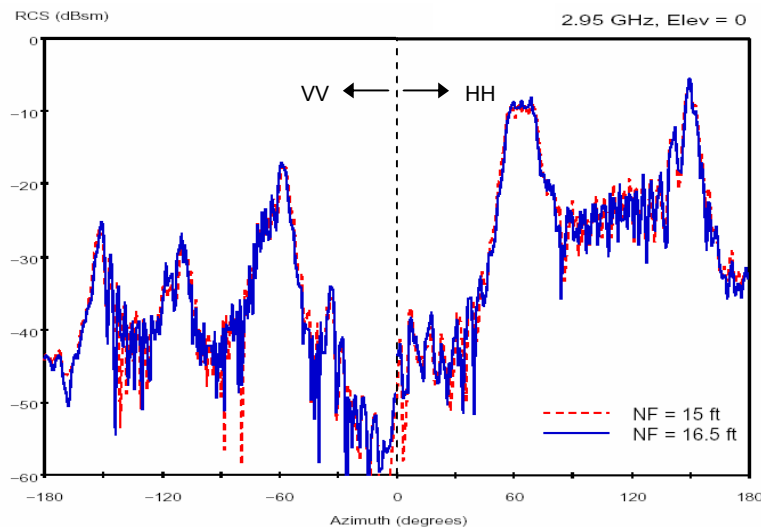
## Predicted Far Field



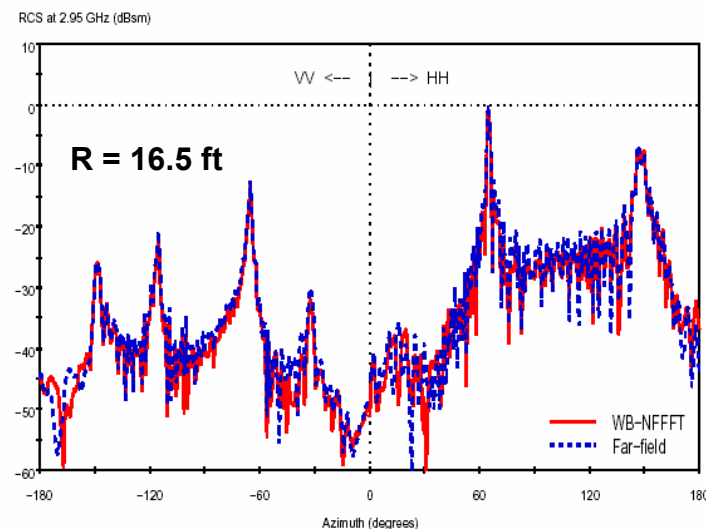
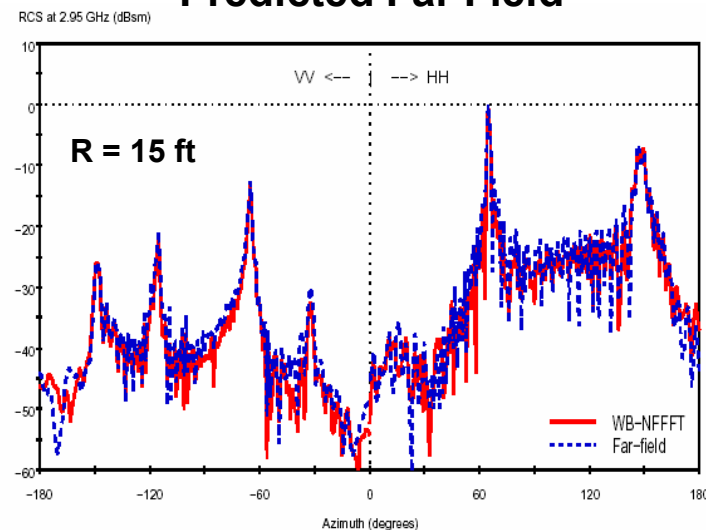
**AFRL “Delta Dart” (D2) test body**  
**1-D CNFFFT (waterline cut)**  
**Frequency = 1.48 GHz**  
**Target size (D) = 6.67 ft. ( $10\lambda$ )**  
**NF standoff (R) = 15, 16.5 ft. ( $2.25D$ ,  $2.5D$ )**

# CNFFFT Example – Measured Data – 3 of 3

## Measured Near Field



## Predicted Far Field



**AFRL "Delta Dart" (D2) test body**  
**1-D CNFFFT (waterline cut)**  
**Frequency = 2.95 GHz**  
**Target size (D) = 6.67 ft. ( $20\lambda$ )**  
**NF standoff (R) = 15, 16.5 ft. ( $2.25D$ ,  $2.5D$ )**

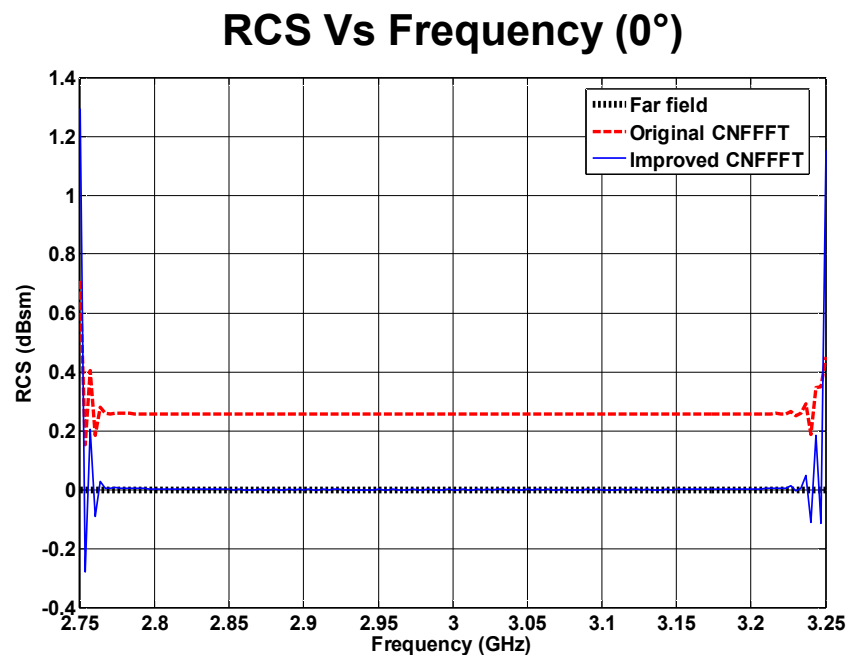
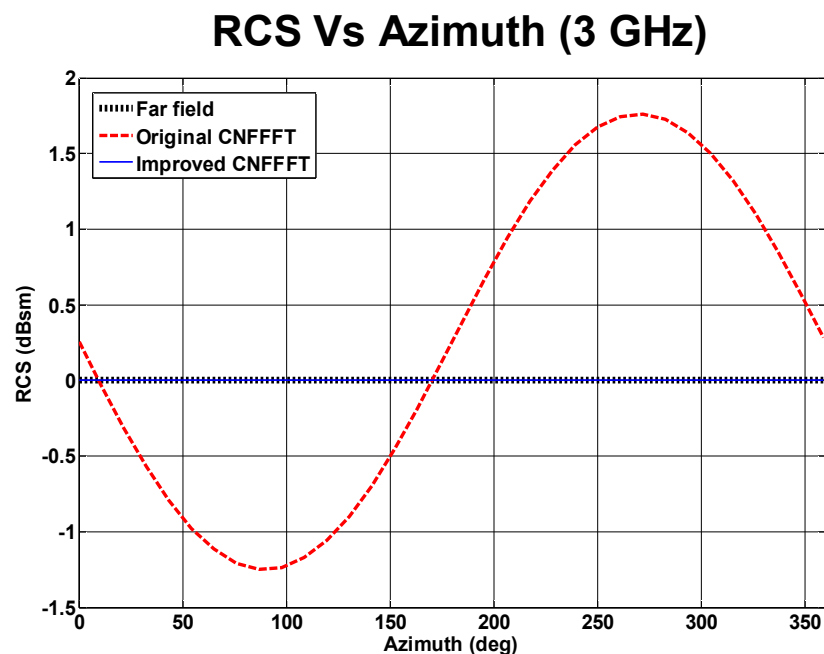


## Appendix 2: CNFFFT Numerical Improvement\* (2005)

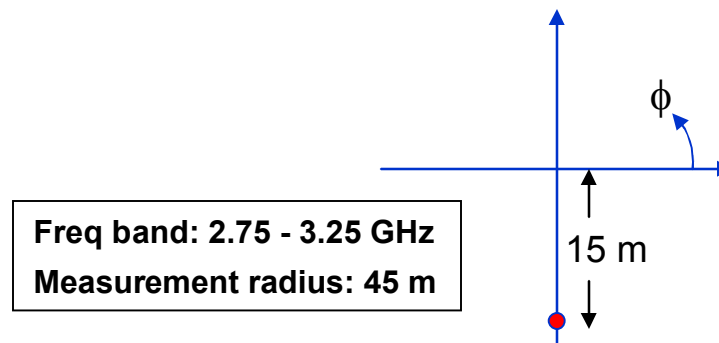
\* LaHaie, I. J., et al. (2005), "An Improved Version of the Circular Near Field-to-Far Field Transformation (CNFFFT)," *Proc. AMTA '05*, pp. 196-201.

# Improved CNFFFT Example Results – 1 of 2

## Numerical Simulations: Single Point Scatterer



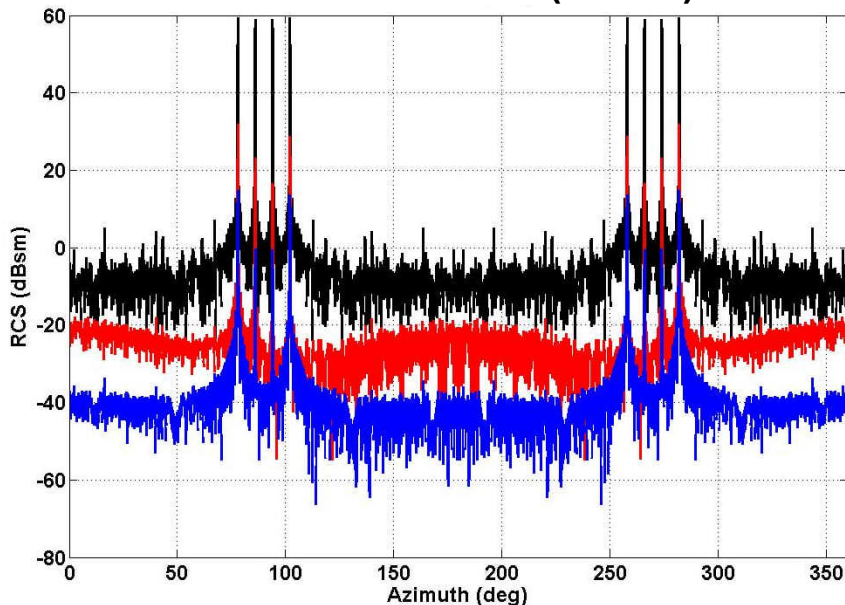
- Recent improvements to CNFFFT reduce algorithm error to essentially zero
  - for targets satisfying the reflectivity model
- Ringing at edges of band are due to finite bandwidth effects of range compensation



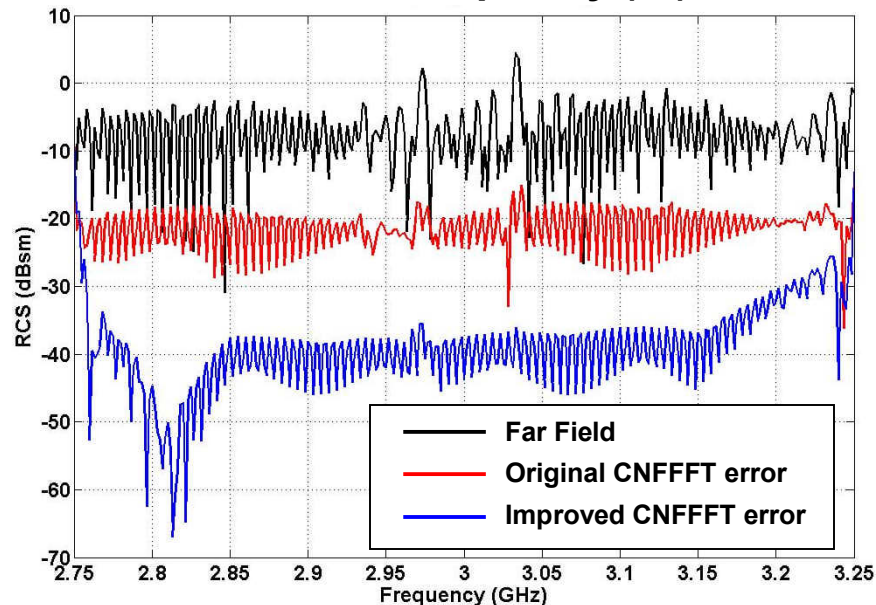
# Improved CNFFFT Example Results – 2 of 2

## Numerical Simulations: X-Wing Target

RCS Vs Azimuth (3 GHz)



RCS Vs Frequency (0°)



- Improvements are less noticeable for a complex target
  - but they can still make a difference when performing RCS diagnostics
- Residual error is ~35 dB below target

